

# Risk of Bitcoin Market: Volatility, Jumps, and Forecasts \*

Junjie Hu<sup>†</sup>, Weiyu Kuo<sup>‡</sup>, Wolfgang Karl Härdle<sup>§</sup>

18.11.2019

## Abstract

Among all the emerging markets, the cryptocurrency market is considered the most controversial and simultaneously the most interesting one. The visibly significant market capitalization of cryptos motivates modern financial instruments such as futures and options. Those will depend on the dynamics, volatility, or even the jumps of cryptos. In this paper, the risk characteristics for Bitcoin are analyzed from a realized volatility dynamics view. The realized variance  $RV$  is estimated with the corrected threshold jump components  $J$ , realized semi-variance  $RSV^{+/-}$ , and signed jumps  $J^{+/-}$ . Our empirical results show that the BTC is far riskier than any of the other developed financial markets. Up to 68% of the days are identified to be entangled with jumps. However, the discontinuities do not contribute to the variance significantly. The full-sample fitting suggests that future  $RV$  has a positive relationship with downside risk and a negative relationship with the positive jump. The rolling-window out-of-sample forecasting results reveal that the forecasting horizon plays an important role in choosing forecasting models. For the long horizon risk forecast, explicitly modeling jumps and signed estimators improve forecasting accuracy and give extra utility up to 19 bps annually, while the HAR model without accounting jumps or signed estimators suits the short horizon case best. Lastly, a simple equal-weighted portfolio of BTC not only significantly reduces the size and quantity of jumps but also gives investors higher utility in short horizon case.

*JEL classification:* C53, E47, G11, G17,

*Keywords:* Bitcoin, Risk Management, Realized Variance, Thresholded Jump, Signed Jumps, Realized Utility

---

\* Supported by Deutsche Forschungsgemeinschaft via IRTG 1792 "High Dimensional Nonstationary Time Series", Humboldt-Universität zu Berlin. All supplementary and Python code can be obtained: [RCVJ\\_Forecasting](#)

<sup>†</sup> Corresponding author. School of Business and Economics, Humboldt-Universität zu Berlin. Dorotheen Str. 1, 10099 Berlin, Germany. Email: [hujunjie@hu-berlin.de](mailto:hujunjie@hu-berlin.de)

<sup>‡</sup> Department of International Business and Risk and Insurance Research Center, National Chengchi University, Taipei City, Taiwan 116. Email: [wkuo@nccu.edu.tw](mailto:wkuo@nccu.edu.tw)

<sup>§</sup> C.A.S.E. - Center for Applied Statistics and Economics, Humboldt-Universität zu Berlin; Sim Kee Boon Institute for Financial Economics, Singapore Management University; Wang Yanan Institute for Studies in Economics, Xiamen University; Department of Mathematics and Physics, Charles University Prague. Email: [haerdle@hu-berlin.de](mailto:haerdle@hu-berlin.de)

# 1. Introduction

Understanding and managing the risk of the cryptocurrency market is crucial for financial investment and construction of contingent claims. The popularity of cryptocurrency investment has been rising along with the discussions on blockchain technology applications, for example, the recent Libra from Facebook. However, many of the investors are not informed or cautious enough about their portfolio risk contributed by cryptocurrency. Different assets may have similar risk characteristics, however, the cryptocurrency can be viewed as an outlier in the sense of increased volatility and more frequent jumps.

Among all the cryptocurrencies, we are motivated to single out the risk of Bitcoin (BTC) for its dominant market share (more than 70%) and active trading. BTC was first proposed by Nakamoto (2008) and then initialized in 2009. It is built on the blockchain technology which decentralizes and distributes information through networks worldwide, thus BTC is a naturally decentralized currency as being part of the blockchain. Nevertheless, regulations can be enforced to the exchanges in which BTC and any other cryptocurrencies are traded. This research uses data from some of the regulated exchanges.

The risk of BTC has been discussed from different angles. Concerning its obvious regulatory risk as an unprecedented "currency" not issued or endorsed by governments, existed literature studies its fundamental risk. Such as, Yermack (2015) argues that BTC is rather a speculative investment than a "currency" because of reasons such as its price is too volatile for users, low acceptance from common merchants, etc. Hafner (2018) and Gerlach et al. (2019) find strong speculative bubble properties in both CRIX (Trimborn and Härdle (2018)) and BTC. Griffin and Shams (2018) document possible price manipulations. Due to the lack of fundamental value, Bukovina et al. (2016); Garcia and Schweitzer (2015); Balcilar et al. (2017) find that the latent drivers of BTC price and volatility could be the sentiment or a series of social signals such as opinions and trading volume. A recent paper of Traian Pele et al. (2019) classify cryptocurrency as a new asset class by its statistical features. Moreover, the risk of BTC is considered from the aspect of portfolio management. BTC is found to function as a hedging or risk haven asset (Bouri et al. (2017); Urquhart and Zhang (2019)) and it has similar properties like gold under the asymmetric GARCH models (Gronwald (2014); Dyhrberg (2016)). Glaser et al. (2014) argue that people use BTC not for transactions but as an alternative investment.

We are motivated to study the volatility of BTC for the reasons as follows. First is the fact that BTC has frequently experienced extreme variance and jumps on price since 2013. The Bitcoin market started to draw attention in 2013 when the unit price exceeded \$100. Four years later, in January 2017, the unit price hit \$1000 and reached almost \$20,000 by

the end of 2017. The bubble burst in 2018, its price dropped around 80% from the peak in one year and it climbed up again in 2019. In our sample period from 2017 to 2019, we observe that the 5-minute logarithmic returns of BTC span from -18.64% up to 8.09%. Secondly, the rapid development of Bitcoin and its derivatives market demand studies on the volatility and jump process. Apart from many of the online exchanges offering BTC futures and options, the strictly regulated exchange CME launched futures on BTC in 2017. More and more investors entering the BTC market cause daily trading volume raising from around \$100M at the beginning of 2017 to approximately \$20,000M in the middle of 2019.<sup>1</sup> And some studies have been carried on those phenomena. A recent study Conrad et al. (2018) decompose the volatility into short term and long term components by GARCH-MIDAS analysis, and study the volatility correlation between BTC and some other indices, for example, Baltic dry index. Scaillet et al. (2018) analyze the jump behavior using the dataset from Mt. Gox exchange in the sample period from 2011 to 2013. And Hou et al. (2018) attempt to calibrate an option pricing model adapting the high volatility and jump properties. Many other papers focus on the forecasting side, for example, Pichl and Kaizoji (2017).

In this paper, we study the Realized Variance ( $RV$ ) which is one of the most important risk measures.  $RV$  which accounts intraday information from high-frequency data, essentially the sum of squared returns over the period, was advocated by previous literature (see e.g Andersen et al. (2001b); Barndorff-Nielsen and Shephard (2002a)). Andersen et al. (2001a) document that this model-free estimate is highly right-skewed, logarithmic normal distributed and characterized by a strong temporal dependency property. In practice, a continuous diffusion sample path assumption rarely holds and discontinuity should be accounted in. We separate jump components  $J$  based on model provided by Barndorff-Nielsen and Shephard (2004). After illustrating the empirical result that the BTC price process suffers from consecutive jumps which cause the jump estimator biased, we correct the bias by employing the thresholded jump estimator from Corsi et al. (2010). Two interesting findings on jump risk are insightful. Firstly, despite the extraordinary amount and large size of jumps being detected in BTC, the discontinuities do not contribute much to risk. Moreover, a simple equal-weighted portfolio of BTC from different exchanges reduces the idiosyncratic jump risk significantly. To further investigate the asymmetric effect, we decompose  $RV$  into upside risk and downside risk, i.e realized semi-variance  $RSV^{+/-}$  (Barndorff-Nielsen et al. (2008b)) and then yield the positive/negative jump components  $J^{+/-}$ .

Under the forecasting setting motivated by Heterogeneous AutoRegression (HAR) in Corsi (2009), we focus on two main issues. The first issue is the relationship between jump

---

<sup>1</sup>Data source: [www.coinmarketcap.com](http://www.coinmarketcap.com)

and semi-variance estimators and future realized variances. Previous literature studies this issue on several different assets, however, obtaining contradictory results. For example, Andersen et al. (2007) find negative relationship between jumps and future  $RV$ , and Corsi et al. (2010) document that the threshold jump estimator has significant positive relationship with future  $RV$ . We find that the coefficients of regressors are evolving systematically by employing a 90-day rolling window forecasting method. Especially, it is worth to notice that during the BTC market crash at the beginning of 2018, the downside variance  $RSV^-$  is positively correlated with future  $RV$  significantly and the positive jump  $J^+$  has a significant negative relationship with  $RV$ . The second issue regards whether and when an investor should explicitly account for jump estimators in the  $RV$  forecasting of BTC. It is a stylized fact that jumps give extra information, Nolte and Xu (2015) conclude that modeling jumps explicitly improves the forecasting. Our out-of-sample forecasting result shows that the necessity of explicitly modeling jump or signed estimators to forecast  $RV$  of BTC heavily relies on the forecasting horizon. Specifically, in the short forecasting horizon,  $h = 1$ , the HAR model with only lagged  $RV$  outperforms all of other models accounted for jump or signed estimators. As the forecasting horizon gets longer,  $h = 30$ , separating jumps improve forecasting accuracy significantly by the D-M test. Such a finding is further confirmed from an economic point of view by a utility-based framework (Bollerslev et al. (2018)).

We will proceed with the article as follows. In section 2, we briefly describe the realized variance and jump estimators used in this article. Then, in section 3, we present the data we use, followed by a discussion on BTC price processes and summary statistics on (semi-)realized variances and jumps. Section 4 discuss the construction and comparison of forecasting models and the forecasts are evaluated under a utility-based framework. Finally, we conclude our findings and remarks in section 5.

## 2. Realized Variance and Jump Estimators

Realized variance and jump modeling have been developed in the recent two decades. In this section, we present the construction of the estimators used in this article. Starting with the Realized Variance  $RV$ , we introduce the Jump component  $J$  separated from  $RV$  by the BiPower Variance  $BPV$ . Then, we correct the bias caused by consecutive jumps by the threshold method. Furthermore, to decompose the jump component into positive and negative  $J^{+/-}$ , we employ the Realized SemiVariance  $RSV^{+/-}$ .

All estimators are constricted in a continuous-time jump diffusion process framework, i.e for a logarithmic asset price  $p(t)$ :

$$dp(t) = \mu(t)dt + \sigma(t)dW(t) + \kappa(t)dq(t), 0 \leq t \leq T \quad (1)$$

where  $\mu(t)$  is a continuous process with bounded local variation,  $\sigma(t)$  is a càdlàg process,  $W(t)$  is Brownian motion. The third term on the right-hand side is the jump process, where  $q$  counts the number of jumps with time-varying intensity denoted by  $\kappa$ .

This article uses logarithmic returns  $r_{t+j\Delta} \stackrel{\text{def}}{=} p(t+j\Delta) - p(t+(j-1)\Delta)$  which denotes the  $j$ -th observed value in day  $t$ , the given sampling step  $\Delta$  will be clarified latter.

## 2.1. Realized Variance and Jump

Realized variance  $RV_{t,t+1}$  is simply the cumulative squared logarithmic returns over time period  $[t, t+1]$ : (For convenience, we omit one  $t$ , i.e  $RV_{t+1} = RV_{t,t+1}$ )

$$RV_{t+1}(\Delta) \stackrel{\text{def}}{=} \sum_{j=1}^{1/\Delta} r_{t+j\Delta}^2 \quad (2)$$

To calculate (2),  $[t, t+1]$  is partitioned into  $N$  intervals evenly. The sampling step is  $\Delta = 1/N$ , for example, with 288 observations each day,  $\Delta = 1/288$ . By the theory of quadratic variation, the increment of Quadratic Variation  $QV$  of  $p(t)$  can be expressed as:

$$\begin{aligned} QV_{t+1} &= \text{p-lim}_{\Delta \rightarrow 0} \sum_{j=1}^{1/\Delta} r_{t+j\Delta}^2 \\ &= \int_t^{t+1} \sigma^2(s)ds + \sum_{t < s \leq t+1} \kappa^2(s) \end{aligned} \quad (3)$$

The variation of  $p(t)$  measured by  $QV$  comes from two sources, one is driven by the càdlàg process and one is caused by the jump process. A series of literature discusses the convergence properties of  $RV$ . Andersen et al. (2001b), Barndorff-Nielsen and Shephard (2002a), Barndorff-Nielsen and Shephard (2002b) document the absence of jumps. Later, Barndorff-Nielsen and Shephard (2004), Barndorff-Nielsen and Shephard (2006), Andersen et al. (2007) generalize to possible jumps.  $RV$  converges in probability to  $QV$  as  $\Delta$  goes to 0:

$$RV_{t+1}(\Delta) \xrightarrow{P} \underbrace{\int_t^{t+1} \sigma^2(s)ds}_{IV_{t+1}} + \underbrace{\sum_{t < s \leq t+1} \kappa^2(s)}_{J_{t+1}} \quad (4)$$

Hence,  $RV$  consists of two components: The continuous  $IV$  component, and the Jump component  $J$ . The BiPower Variation  $BPV$  measuring the continuous process allows separating the components

$$BPV_{t+1}(\Delta) = \mu_1^{-2} \sum_{j=2}^{1/\Delta} |r_{t+j\Delta}| \cdot |r_{t+(j-1)\Delta}|, \quad (5)$$

where  $\mu_1 = \sqrt{2/\pi}$ .  $BPV$  converges in probability to  $IV$  in (4) as  $\Delta$  goes to 0. Intuitively,  $BPV$  is robust to an infrequent jump process as it is smoothed by cumulating the adjacent logarithmic returns.  $J$  can, therefore, be isolated by taking the difference of  $RV$  and  $BPV$ . And then the difference is truncated to guarantee that  $J$  is non-negative, see (6).

$$\begin{aligned} BPV_{t+1}(\Delta) &\xrightarrow{P} \int_t^{t+1} \sigma^2(s) ds \\ RV_{t+1}(\Delta) - BPV_{t+1}(\Delta) &\xrightarrow{P} \sum_{t < s \leq t+1} \kappa^2(s) \\ J_{t+1} &\stackrel{\text{def}}{=} \max \{RV_{t+1}(\Delta) - BPV_{t+1}(\Delta), 0\} \end{aligned} \quad (6)$$

## 2.2. Threshold Bipower Variance and Jump

$BPV$  is effective in the sense of smoothing a variation process when both size and quantity in the jump process are relatively small, in other words,  $BPV$  is biased to large and consecutive jumps which are not evidently appropriated for investigating cryptocurrencies.

For example, Fig.1 shows that consecutive jumps occurred in case the variation process is not smoothed by  $BPV$ . We can observe three big price jumps on 17th May 2019, consecutively, around 3 in the morning (GMT), however, the annualized  $RV = 6.09$  and  $BPV = 6.44$  imply that no jump happened during that day.

We correct such bias by implementing the threshold variation model. The main idea of Thresholded MultiPower Variation  $TMPV$  is documented in Mancini (2009) which essentially truncates any logarithmic return when it exceeds a certain level of  $\theta$ . At time point  $t+j\Delta$ , the threshold value  $\theta_{t+j\Delta}$  is varying along with local variance  $\widehat{V}_{t+j\Delta}$  for given constant coefficient, i.e  $\theta_{t+j\Delta} = c_\theta^2 \cdot \widehat{V}_{t+j\Delta}$ . Corsi et al. (2010) show that any unbiased estimator for realized local variance  $\sigma^2$  can be implemented, e.g the Fan and Yao (2008) estimator we use detailed in Appendix B.1 which is essentially a kernel smoothing estimator. The constant  $c_\theta$  also impacts  $TMPV$ , i.e as  $c_\theta$  goes larger,  $TMPV$  truncates less values. In our main empirical results, we follow the literature and choose  $c_\theta = 3$ . After the estimation of threshold value  $\theta_{t+j\Delta}$ , one can directly truncate the returns exceeded the threshold. However, this

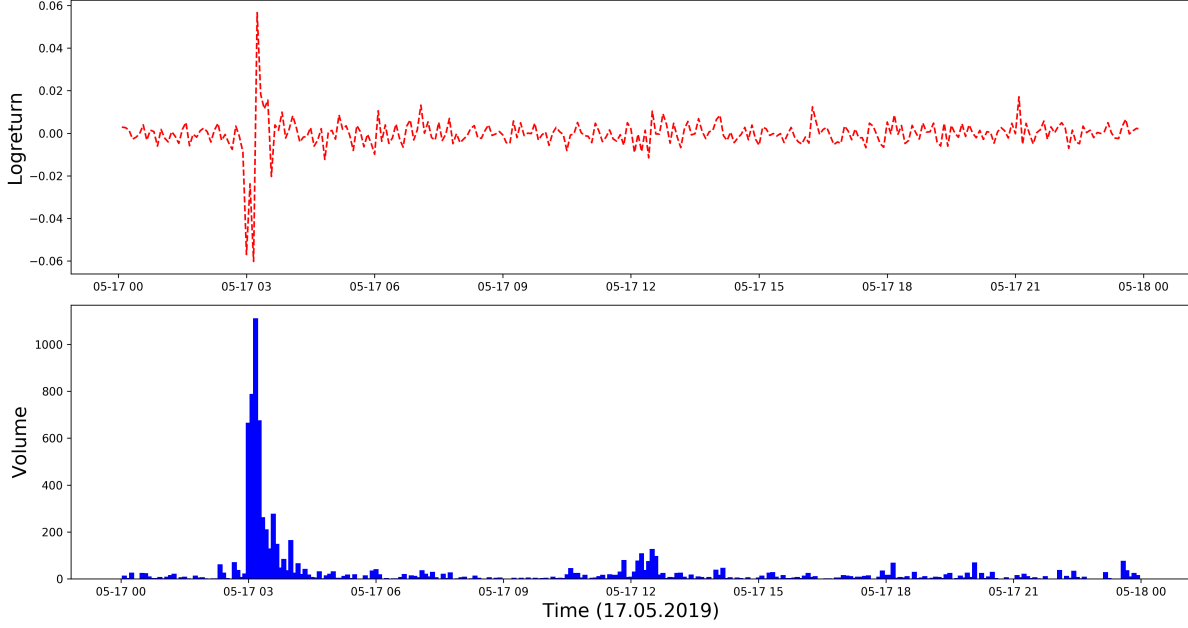


**Fig. 1:** *BPV* is biased to consecutive jumps: A trajectory of the intraday behavior of BTC-G, 17th May 2019.  $RV = 6.09$ ,  $BPV = 6.44$  imply that no jump has happened in this day. Upper panel shows the logarithmic return process and the bottom panel is the corresponding trading volume. Both in 5-minute sampling frequency.

could also annihilate some of the price changes for *TBPV* that are not "real" jumps which in turn cause more "fake" jumps been detected. Hence, we implement the corrected version of *TMPV* that relieves the "double-sword" bias (Corsi et al. (2010)). To avoid confusion, *TMPV* is short for the corrected version of *TMPV* hereafter.

Essentially, instead of eliminating every of the points that has square-returns  $r_{t+j\Delta}^2$  larger than certain threshold value  $\theta_{t+j\Delta}$ , the corrected *TMPV* replaces the  $\eta$ -th power logarithmic return  $|r_{t+j\Delta}|^\eta$  with  $r^e(\theta_{t+j\Delta}, \eta)$  which is the expected value under assumption that  $r_{t+j\Delta} \sim N(0, \sigma^2)$ . The conditional replacement logarithmic return  $C_\eta(r_{t+j\Delta}, \theta)$  can be written as:

$$C_\eta(r_{t+j\Delta}, \theta_{t+j\Delta}) = \begin{cases} |r_{t+j\Delta}|^\eta & , r_{t+j\Delta}^2 \leq \theta \\ r^e_{t+j\Delta}(\theta_{t+j\Delta}, \eta) & , r_{t+j\Delta}^2 > \theta \end{cases} \quad (7)$$

More details about expected logarithmic return  $r^e_t(\theta_t, \eta)$  is documented in Appendix B.2.

Similar to procedure for detecting  $J$ , two special cases of *TMPV* are used here. *TBPV* estimates  $\int_t^{t+1} \sigma^2(s)ds$  and *TTPV* estimates  $\int_t^{t+1} \sigma^4(s)ds$ . Two estimators are defined as follows.

$$TBPV_{t+1}(\Delta) = \mu_1^{-2} \cdot \sum_{j=2}^{1/\Delta} C_1(r_{t+j\Delta}, \theta_{t+j\Delta}) C_1(r_{t+(j-1)\Delta}, \theta_{t+(j-1)\Delta}) \quad (8)$$

$$\begin{aligned} TTPV_{t+1}(\Delta) &= \mu_{\frac{4}{3}}^{-3} \cdot \Delta^{-1} \cdot \sum_{j=3}^{1/\Delta} C_{\frac{4}{3}}(r_{t+j\Delta}, \theta_{t+j\Delta}) \\ &\quad \cdot C_{\frac{4}{3}}(r_{t+(j-1)\Delta}, \theta_{t+(j-1)\Delta}) \\ &\quad \cdot C_{\frac{4}{3}}(r_{t+(j-2)\Delta}, \theta_{t+(j-2)\Delta}) \end{aligned} \quad (9)$$

Test for thresholded jumps  $t$ - $z$  is given by (10), provided by Corsi et al. (2010) which is based on the ratio statistic from Huang and Tauchen (2005), detailed in Andersen et al. (2007) under continuous jump diffusion model. Where  $\zeta = \frac{\pi^2}{4} + \pi - 5$ . Under a series assumptions, for the null hypothesis that no jump exists,  $t$ - $z$  converges to standard normal distribution as  $\Delta$  goes to 0, i.e  $t$ - $z \xrightarrow{\mathcal{L}} N(0, 1)$ .

$$t\text{-}z_{t+1} = \frac{\{RV_{t+1}(\Delta) - TBPV_{t+1}(\Delta)\} RV_{t+1}^{-1}(\Delta)}{\sqrt{\Delta \cdot \zeta \cdot \max\left\{1, \frac{TTPV_{t+1}(\Delta)}{\{TBPV_{t+1}(\Delta)\}^2}\right\}}} \quad (10)$$

Then, we redefine the corrected version of realized Jumps  $J$  taking account only the significant jumps by  $t$ - $z$  test.

$$J_{t+1}(\Delta) \stackrel{\text{def}}{=} \max\{RV_{t+1}(\Delta) - TBPV_{t+1}(\Delta), 0\} \cdot \mathbf{I}\{t\text{-}z_{t+1} > \Phi_{\alpha}^{-1}\} \quad (11)$$

Consequently, we can enforce the  $RV = C + J$  by defining continuous component  $C_{t+1}(\Delta) \stackrel{\text{def}}{=} RV_{t+1}(\Delta) - J_{t+1}(\Delta)$ .

### 2.3. Realized Semivariance and Signed Jumps

In this subsection, we go further to discuss the detection of positive and negative jumps. Recall that under the continuous jump diffusion model assumption, the jump component of quadratic variation  $QV_{t+1}$  is the accumulated sum of squared infinitesimal changes  $\Delta p_s = p_s - p_{s-}$ , i.e  $\sum_{t < s \leq t+1} (\Delta p)^2(s)$ . Hence, the jump component is guaranteed to be non-negative as defined in (11). On the other hand, from the finance perspective, investors are keen to understand the dynamics of the positive and negative jump, especially how those estimators impact the market of their interests. For example, the asymmetric effect of positive and negative risk on asset returns is well investigated in previous literature.

Realized semivariance  $RSV$  (Barndorff-Nielsen et al. (2008b)) provides us one way to



separate positive and negative jumps from the realized variance process. The definition of positive (negative)  $RSV^{+(-)}$  shown in (12) is essentially the the sum of the squared positive (negative) logarithmic returns.

$$RSV_{t+1}^{+(-)} = \sum_{j=1}^{1/\Delta} r_{t+j\Delta}^2 \cdot \mathbf{I}\{r_{t+j\Delta} > (<)0\} \quad (12)$$

It is straight forward that  $RV$  can be decomposed into  $RSV^+$  and  $RSV^-$  completely, i.e  $RV = RSV^+ + RSV^-$ , for both finite sample and large sample cases. As sampling frequency  $1/\Delta$  goes infinite, the limiting behavior of  $RSV$  given by (13) under infill asymptotics shows that  $RSV^{+(-)}$  converges to one-half of the integrated variance and positive (negative) sum of squared jumps. For example,

$$RSV_{t+1}^+ \xrightarrow{p} \underbrace{\frac{1}{2} \int_t^{t+1} \sigma^2(s) ds}_{\frac{1}{2}IV_{t+1}} + \underbrace{\sum_{t < s \leq t+1} (\Delta p_s)^2 \cdot \mathbf{I}\{\Delta p_s > 0\}}_{J_{t+1}^+}. \quad (13)$$

With this convergence property above and the property of  $BPV$  described in (6), one can easily separate the Positive (Negative) Jumps  $J^{+(-)}$  by subtracting  $RSV^{+(-)}$  by  $TBPV$ . As defined in (14).

$$J_{t+1}^{+(-)} \stackrel{\text{def}}{=} \max \left\{ RSV_{t+1}^{+(-)} - \frac{1}{2}TBPV_{t+1}, 0 \right\} \quad (14)$$

### 3. Data and Preliminary Analysis

We construct two price processes from two data sources to highlight the robustness of our empirical results on the risk of Bitcoin which is traded among many online exchanges. This section can be roughly divided into 3 parts. We start by introducing our dataset and relevant preprocessing, followed by the discussion on the characteristics of the two price processes. Finally, we present the summary statistics of realized variance and jump components.

#### 3.1. Data Source

There are 254<sup>2</sup> online exchanges trading various types of cryptocurrencies and each of the coins is traded in different exchanges globally. Among all crypto markets, the Bitcoin market is dominant with more than 70% market share. In this article, we focus only on the Bitcoin market, two price processes constructed from two different data sources are

---

<sup>2</sup>Until July 2019, <https://coin.market/exchanges-info.php>

studied. One process is provided by a private data company DYOS<sup>3</sup>, hereafter **BTC-D**. And the other one is obtained from an online free provider<sup>4</sup>, hereafter **BTC-G**. BTC-D price is equal-weighted prices from three actively trading exchanges, Poloniex, Bittrex, and Bitfinex<sup>5</sup>. Such construction can be viewed as the price of a portfolio, which allows investors to diversify idiosyncratic risk from exchanges. In contrast, BTC-G price comes from only one exchange, Gemini<sup>6</sup>, which is one of the largest digital exchanges regulated by NYDFS<sup>7</sup>.

Although the full dataset can be dated back to 2014, the trading was not active until 2017. We thus construct our data from January 2017. In particular, the sample period of BTC-D price is from January 2017 to May 2019, while that of BTC-G price starts from January 2017 to July 2019. The Bitcoin market is trading all-day and all-year globally akin to the foreign exchange market which prompts the issue of removing the illiquidity periods, such as weekends/holidays, and inactive trading hours. In this article, we do not remove any trading days because many of the non-institutional investors who can trade during non-business days in the cryptocurrency market. Moreover, as the trading records come from U.S based and Asia based online exchanges, we define the day as 0:00 GMT to 23:55 GMT and keep the whole 24-hour data samples. After cleaning and removing the trading days that have an incomplete number of samples, the dataset has an 864-day sample for BTC-D and an 883-day sample for BTC-G. Note that due to the data missing problem from BTC-G datasource, we remove samples from 15th Nov. 2018 to 6th Dec. 2018. Both two data sources are sampled every 5-min, thus every day has 288 samples.

### 3.2. *Price Process of BTC*

A series of literature has discussed sampling frequency issues regarding realized variance estimator impaired by microstructure noise, e.g Ait-Sahalia et al. (2005) and Bandi and Russell (2008) attempt to derive optimal sampling frequency by explicitly assuming noise structure, Zhang et al. (2005) Zhang (2006) document the efficient estimator by subsampling schemes, and kernel methods are introduced to handle the noise (Barndorff-Nielsen et al. (2008a); Hansen and Lunde (2006)). Liu et al. (2015) test estimators constructed with different sampling frequency and find no evidence against the 5-minute sampling strategy. Following most of the empirical literature such as Andersen et al. (2001a); Andersen et al. (2007), we adopt the 5-minute high-frequency sampling strategy for both BTC-D and BTC-G, i.e taking the transaction prices closest to the end of each 5-minute interval to calculate

---

<sup>3</sup>Dyos solutions GmbH, Berlin, Germany

<sup>4</sup><https://www.cryptodatadownload.com/>

<sup>5</sup>Poloniex and Bittrex are U.S based companies, and Bitfinex located in Hongkong

<sup>6</sup><https://gemini.com/about/>

<sup>7</sup>New York State Department of Financial Services

5-minute returns.

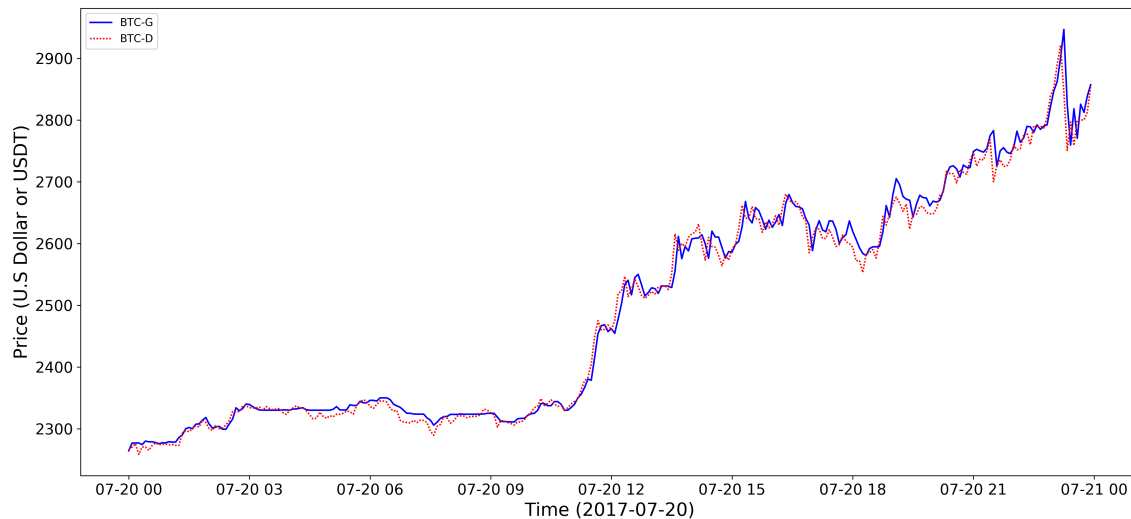


**Fig. 2:** Price trajectory of **BTC-D** (dash line) and **BTC-G** (solid line) in the highest accumulated logreturn day, 20th July, 2017. [RiskBTC](#)

Like fiat currencies, the price of BTC is essentially an exchange rate against another currency. In most of the exchanges, there are two notions of BTC price. BTC price can be denoted by either U.S dollar or another cryptocurrency named USDT which claims to tether U.S. dollar with a 1:1 exchange rate.

The price in BTC-D is denoted by USDT, while the prices of BTC-G come from U.S. dollars trades. Fig.2 shows the realized sample trajectory of BTC-D and BTC-G evolving closely in an extremely volatile day. The correlation between the daily logarithmic returns of the two datasets is around 98.2%.

### 3.3. Dynamics of Realized Variance Estimators

This subsection discusses the dynamics of variance estimates in three aspects including descriptive statistics, empirical distribution, and series autocorrelation.

The extremely high risk of BTC comparing with tradition asset stands out immediately by the sample mean of  $RV$  shown in Table 1. For example, the sample mean of annualized daily realized variance of BTC-D is 1.16. In contrast, one of the most volatile equity market indices, SSEC, has annualized daily realized variance 0.23.<sup>8</sup> More comparisons are detailed in Appendix A.1.

---

<sup>8</sup>Datasource from Realized Library, Oxford-Man Institute of Quantitative Finance. The trading hour bias is corrected by accounting the overnight price change (Bollerslev et al. (2018)) to allow the two  $RV$  estimators to be comparable.

The descriptive statistics of continuous component  $C$  in Table 1 suggest that the discontinuities do not contribute to the risk too much. As definition in section 2.2,  $C$  is the difference between  $RV$  and  $J$  which implies closer the distance between  $C$  and  $RV$ , lower the contribution from  $J$ . On average, jumps contribute to risk up to 6.8%<sup>9</sup> for BTC-D, and up to 17.2% for BTC-G. And ADF unit root test suggests that most estimators do not contain unit root at 5% significant level.

**Table 1:** Summary Statistics For Bitcoin Annualized Daily (Semi-)Realized Variance

| <b>Panel A: BTC-D</b> |         |         |          |            |               |               |         |
|-----------------------|---------|---------|----------|------------|---------------|---------------|---------|
|                       | $RV$    | $RSV^+$ | $RSV^-$  | $\log(RV)$ | $\log(RSV^+)$ | $\log(RSV^-)$ | $C$     |
| mean                  | 1.16    | 0.57    | 0.59     | -0.60      | -1.32         | -1.30         | 1.08    |
| std                   | 2.05    | 1.02    | 1.05     | 1.20       | 1.22          | 1.23          | 2.01    |
| min                   | 0.02    | 0.01    | 0.01     | -3.98      | -4.88         | -4.51         | 0.01    |
| max                   | 26.07   | 13.28   | 12.80    | 3.26       | 2.59          | 2.55          | 26.07   |
| skewness              | 5.59    | 5.78    | 5.41     | 0.06       | 0.04          | 0.10          | 5.73    |
| kurtosis              | 43.38   | 46.24   | 40.12    | -0.04      | -0.03         | -0.15         | 45.86   |
| acf(1)                | 0.53    | 0.51    | 0.52     | 0.79       | 0.78          | 0.77          | 0.56    |
| acf(7)                | 0.17    | 0.16    | 0.17     | 0.58       | 0.58          | 0.57          | 0.18    |
| acf(30)               | 0.11    | 0.10    | 0.11     | 0.38       | 0.37          | 0.38          | 0.13    |
| acf(100)              | 0.06    | 0.06    | 0.06     | 0.23       | 0.23          | 0.23          | 0.07    |
| ADF                   | -3.16** | -3.22** | -3.12**  | -4.36***   | -4.34***      | -4.42***      | -3.10** |
| <b>Panel B: BTC-G</b> |         |         |          |            |               |               |         |
|                       | $RV$    | $RSV^+$ | $RSV^-$  | $\log(RV)$ | $\log(RSV^+)$ | $\log(RSV^-)$ | $C$     |
| mean                  | 0.93    | 0.45    | 0.49     | -0.92      | -1.66         | -1.64         | 0.77    |
| std                   | 1.76    | 0.84    | 0.98     | 1.32       | 1.32          | 1.37          | 1.55    |
| min                   | 0.01    | 0.00    | 0.00     | -4.88      | -5.51         | -5.63         | 0.00    |
| max                   | 21.99   | 11.78   | 14.52    | 3.09       | 2.47          | 2.68          | 21.99   |
| skewness              | 5.86    | 6.32    | 6.85     | -0.04      | -0.04         | -0.01         | 6.21    |
| kurtosis              | 47.28   | 59.42   | 68.92    | -0.10      | -0.14         | -0.19         | 57.88   |
| acf(1)                | 0.42    | 0.45    | 0.35     | 0.74       | 0.73          | 0.71          | 0.50    |
| acf(7)                | 0.13    | 0.14    | 0.11     | 0.49       | 0.51          | 0.47          | 0.19    |
| acf(30)               | 0.09    | 0.09    | 0.07     | 0.26       | 0.26          | 0.25          | 0.14    |
| acf(100)              | 0.03    | 0.04    | 0.02     | 0.11       | 0.11          | 0.11          | 0.04    |
| ADF                   | -3.03** | -3.12** | -4.89*** | -5.06***   | -3.61***      | -5.27***      | -2.77*  |

Panel A and panel B are the descriptive statistics of BTC-D and BTC-G. The left three columns are realized variance, positive realized semi-variance, negative realized semi-variance, followed by the logarithmic form of those three estimators. The right column is the continuous component defined as the difference between realized variance and significant jump. The first six rows for each panel contain the sample mean, standard deviation, sample minimum, maximum, skewness, and excess kurtosis, followed by four autocorrelation with 1-day, 7-day, 30-day, and 100-day lags. the last row reports the Augmented Dickey-Fuller test with three significance levels. \*\*\*: 1% significance, \*\*: 5% significance, \*: 10% significance.

Fig. 3 shows two of the most important properties for  $RV$ , the log-normal distribution and strong temporal dependency. We use Epanechnikov kernel with bandwidth=1.5 to estimate the density of logarithmic form of  $RV$ ,  $RSV^{+(-)}$ , and  $C$ . Consistent with the

<sup>9</sup>The average annualized daily  $RV$  is around 1.16, and the average annualized daily jump intensity  $J$  is around 0.08, hence the contribution from jump to risk is around  $0.08/1.16 = 6.8\%$ , likewise for BTC-G.

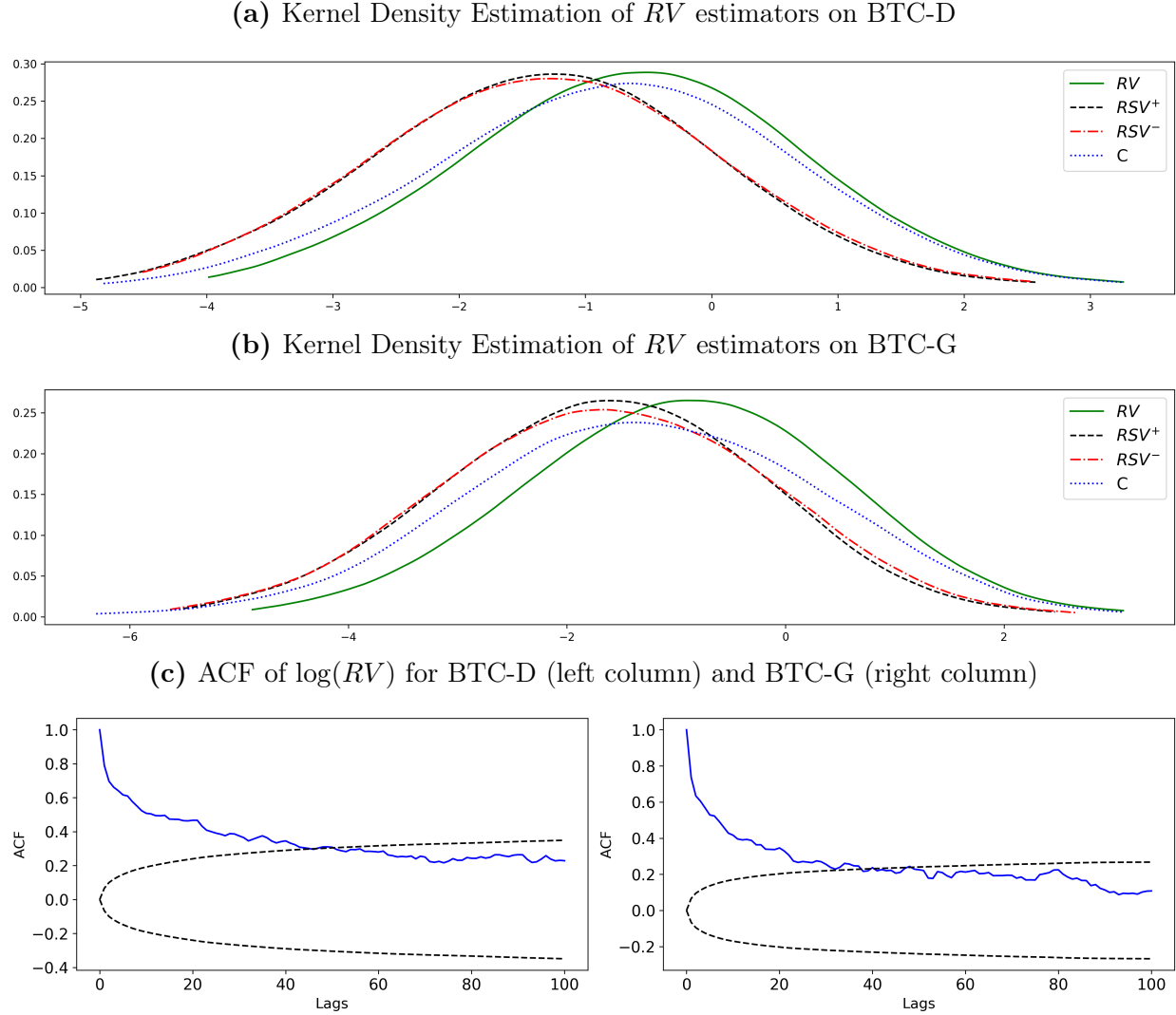


**Fig. 3:** The top two panels are the kernel density estimation on annualized unconditional daily logarithmic estimators for BTC-D (a) and BTC-G (b). Logarithmic estimators in each panel include  $RV$ ,  $RSV^+$ ,  $RSV^-$ , and  $C$ . The last panel is the autocorrelation function of BTC with 95% confidence band. RiskBTC

results that skewness and excess kurtosis of those estimators in logarithmic forms in Table 1, we can see that the  $RV$  can be well approximated by a log-normal distribution. The strong and persistent temporal dependency of  $\log(RV)$  process which can be well described as a long-memory process documented in Andersen et al. (2001a) motivates our forecasting model construction. The ACF statistics in Table 1 in line with the bottom panel in Fig. 3 show that the  $\log(RV)$  processes of both BTC-D and BTC-G have strong temporal dependency. However, the decay of such dependency is much slower in BTC-D than in BTC-G which suggests that one could possibly improve the forecasts by diversifying the BTC investment into different online exchanges.

### 3.4. Dynamics of Jumps Processes

Recall that we construct three jump estimators, the corrected thresholded jump  $J$ , and positive(negative) thresholded jump  $J^{+(-)}$  in Section 2. We first explain the descriptive statistics of the three jump estimators and then show the detected jump processes. Only the non-zero detected jumps are reported in Table 2 and estimator  $J(\alpha)$  is evaluated at 99.99% confidence level.

Jumps appear far more frequently in the Bitcoin market than in any other developed markets comparing our results with the those documented in pervious researches using similar approaches. From our empirical results in Table 2, 39% and 68% of days are detected with jumps for BTC-D and BTC-G, respectively. Corsi et al. (2010) show that for the most liquid six stocks of S&P500, 8.3% of the 1256 sample days are entangled with jumps by the corrected thresholded jump estimator  $J(\alpha = 99.9\%)$ . Andersen et al. (2007) examine on various financial assets including DM/\$, S&P 500 and U.S T-Bond, the result shows that up to 8.3% of all the sample days are detected with jumps in DM/\$ exchange rate market.

Nevertheless, we find that a simple equal-weighted portfolio, BTC-D, reduces the size and quantity of jumps significantly, i.e the jump risk of BTC can be diversified. Comparing the two panels in Table 2, given the same time period and the same jump detection estimator, BTC-D has much fewer sample days contained with price jumps, e.g by  $J(\alpha)$  estimator, 39% of days in BTC-D while 68% of days in BTC-G are found with jumps. The price process of BTC-D is constructed by weighting prices from multiple exchanges equally, thus idiosyncratic jumps from one exchange detected by high-frequency data can be canceled out from such construction. BTC-G is more positive skewed and leptokurtic than BTC-D in terms of all jump estimators which indicates that more extreme jumps appear in BTC-G, for example,  $skewness(\text{BTC-D}, J) = 7.28$  versus  $skewness(\text{BTC-G}, J) = 14.40$  and  $kurtosis(\text{BTC-D}, J) = 73.22$  versus  $kurtosis(\text{BTC-G}, J) = 259.24$ .

The detected jumps processes are shown in Fig. 4. On one hand, from the second figure in each panel of positive and negative jump processes, one can see that the jumps appear more frequently comparing the first figure of such panel, e.g for BTC-D 76% of the sample days are detected with positive jumps, however, only 39% of them are categorized as jump days (See Table 2). On the other hand, the decomposition of  $J(\alpha)$  into signed jump estimators is clean in terms of jump intensity. The average intensity of jump components decomposition is approximate  $J(\alpha) \approx J^+ + J^-$ . This conflict is partially caused by the lack of significance test on signed jumps  $J^{+/-}$ . Also, The size and quantity of negative jumps  $J^-$  are almost equal to that of positive jump  $J^+$  which implies that a jump is not necessary a crash event in the sample period used in this article.

Jumps are usually considered as results from exogenous shocks, for example, the news

**Table 2:** Summary Statistics For BTC Jump Components

|                    | Panel A: BTC-D |       |        | Panel B: BTC-G |       |        |
|--------------------|----------------|-------|--------|----------------|-------|--------|
|                    | $J(\alpha)$    | $J^+$ | $J^-$  | $J(\alpha)$    | $J^+$ | $J^-$  |
| prop. <sup>†</sup> | 0.39           | 0.76  | 0.79   | 0.68           | 0.83  | 0.87   |
| mean               | 0.20           | 0.09  | 0.11   | 0.24           | 0.11  | 0.15   |
| std                | 0.40           | 0.21  | 0.25   | 0.76           | 0.23  | 0.56   |
| skewness           | 7.28           | 5.80  | 9.46   | 14.40          | 6.77  | 17.33  |
| kurtosis           | 73.22          | 43.31 | 131.43 | 259.24         | 62.06 | 368.50 |
| min(%)             | 0.92           | 0.02  | 0.03   | 0.34           | 0.00  | 0.02   |
| 50%                | 0.09           | 0.03  | 0.04   | 0.11           | 0.04  | 0.05   |
| max                | 5.09           | 2.36  | 4.39   | 15.14          | 2.86  | 12.87  |

Panel A and panel B document the descriptive statistics of three jump estimators of BTC-D and BTC-G. Columns from left to right are the corrected thresholded jump estimator  $J(\alpha)$  at  $\alpha = 99.99\%$  confidence level, the thresholded positive jump estimator  $J^+$ , and the thresholded negative jump estimator  $J^-$ . The threshold constant coefficient  $c_\theta = 3$ . The first row reports the proportion of non-zero jumps. The last first rows contain the sample mean, sample deviation, sample minimum, 50% quantile, and sample maximum.

shocks on the financial market. To check the sanity of the detected jumps, we try to link the news and reports to the detected jumps by exemplifying some of the large jumps. We choose four of the days detected with large price jumps marked in the first figure of the upper panel in Fig. 4. The largest detected jump happened in our sample period is 10th March 2017, in which the Bitcoin ETF from Winklevoss twins was denied by the Securities Exchange Commission (SEC).<sup>10</sup> On 29th November 2017, BTC reached \$10,000 where many analysts suspected that the market would be more volatile caused by the profit-taking investors.<sup>11</sup> A mysterious bull run appeared on 12th April 2018 and the BTC price hit \$8,011 from \$6,780 in a short time.<sup>12</sup> Drastic fluctuation happened on 15th October 2018. The BTC price first surged from \$6,376 to \$7,083 and then fell back to \$6,821.<sup>13</sup>

## 4. Accounting Separated Jumps in Realized Variance Modelling

In this section, we study the forecasting of realized variance incorporating with jumps. We first introduce the forecasting models based on Heterogenous Autoregression (HAR), followed by the analysis of the in-sample forecasting results. Then, we construct the adaptive forecasting models and compare the forecasting accuracy. Finally, the realized variance forecasts are evaluated under a utility-based framework for validating our findings in the

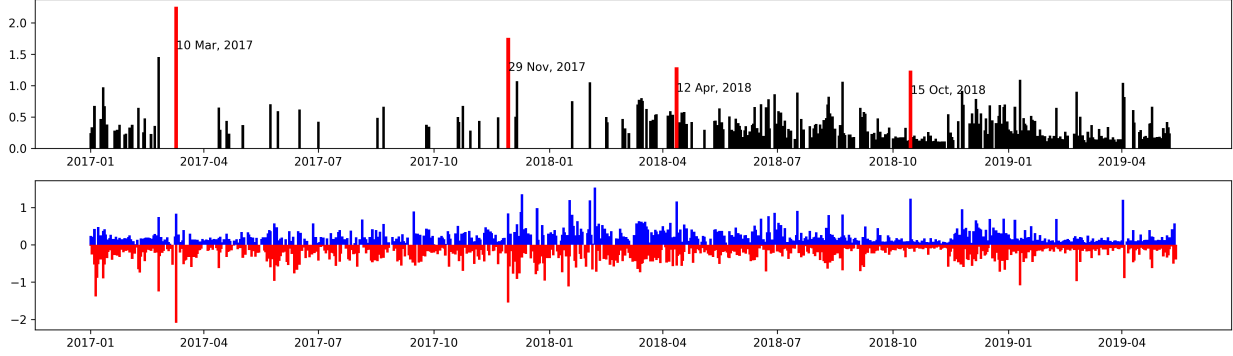
<sup>10</sup>"Breaking: ETF Denied, Bitcoin Price Drops From \$1350 to \$980 Within Hours" from <https://cointelegraph.com/>

<sup>11</sup>Source by: <https://www.fintechfutures.com/>

<sup>12</sup><https://www.investopedia.com/news/why-did-bitcoin-jump-1k-april-12/>

<sup>13</sup><https://medium.com/@bitcurate/>

(a) Jump Process of BTC-D,  $\sqrt{J(\alpha)}$ ,  $\sqrt{J^+}$ , and  $-\sqrt{J^-}$



(b) Jump Process of BTC-G,  $\sqrt{J(\alpha)}$ ,  $\sqrt{J^+}$ , and  $-\sqrt{J^-}$

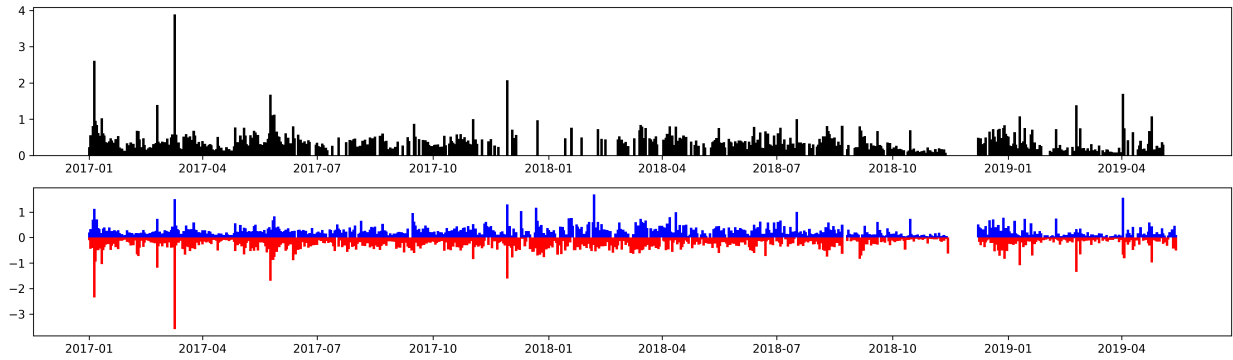


**Fig. 4:** The detected jump estimators of BTC-D (top panel) and BTC-G (bottom panel) evolve over time. The first figure of each panel is the square root form of  $J(\alpha)$  at  $\alpha = 99.99\%$  confidence level. The second figure of each panel contains the square root of the positive jump  $J^+$  and the negative jump  $J^-$ . RiskBTC

economic sense.

#### 4.1. Realized Variance Forecasting Models

In section 2, we illustrate the estimators used in this article including the realized (semi-)variance  $RV$ ,  $RSV^{+/-}$  and three of the jump estimators  $J^{+/-}$ . Before proceeding to the forecasting models, we first clarify the notation of each estimator.

Following the existed literature, *any of the estimators* used here, for example, the estimated realized variance  $RV_{\tau_1, \tau_2}$ , is computed by averaging its daily estimate over time period  $[\tau_1, \tau_2]$ . Let the estimated annualized daily realized variance be  $RV_\tau$ , its corresponding average estimator is defined as:

$$RV_{\tau_1, \tau_2} = \frac{1}{\tau_2 - \tau_1} \sum_{\tau=\tau_1+1}^{\tau_2} RV_\tau \quad (15)$$

The averaging method not only has incorporated information over the period but also



ensure estimates having the same scale. We specially denote the daily lagged, weekly lagged and monthly lagged estimators for further use in (16). As BTC is a 24-hour/7-day trading asset, we use 7 days and 30 days for weekly and monthly estimators instead of 5 days and 20 days. Those three stepwise estimators will then be employed in the latter HAR model which captures the footprint of  $RV$ 's long memory property.

$$\begin{aligned}
&\text{Daily lagged estimator, } RV_D \stackrel{def}{=} RV_{t-1,t} \\
&\text{Weekly lagged estimator, } RV_W \stackrel{def}{=} RV_{t-7,t-1} \\
&\text{monthly lagged estimator, } RV_M \stackrel{def}{=} RV_{t-30,t-7}
\end{aligned} \tag{16}$$

Furthermore, as shown in 3.3, the logarithmic form of realized variance has a stronger temporal dependency and is approximately normal distributed, we transform the estimators into logarithmic form  $\log(RV)$  to incorporate nonlinearity while still keep the model simple. As the square form,  $RV$  is of our interest, any of the forecasting results computed from the logarithmic form is transformed back to square form for comparison purposes.

In the above text, we take the realized variance estimator  $RV$  as an example, the realized semi-variance  $RSV$  and jump  $J^{+/-}$  estimators also follow the notations.

The temporal dependence structure of the realized variance process is crucial in forecasting. Many of the studies use different ARCH, ARMA, and stochastic volatility models to capture the temporal dependency or long-memory effect. Other than those complicated models, a simple linear model named the Heterogenous AutoRegression model, HAR, is proposed in Corsi (2009). The advantages of HAR can be illustrated threefold. First, it is a parameter parsimonious volatility regression model that can be constructed easily with different lagged regressors. Second, it captures the strong temporal dependency and shows good forecasting performance comparing with those complicated models. Finally, HAR can be extended by using any other relevant estimators, for example, the jump components. Such extensibility allows one to investigate a wide range of effects on  $RV$ .

The basic **HAR** model is formulated in (17). As we use the logarithmic form of all estimators, we are essentially estimating the log-log HAR model. The dependent variable  $\log(RV_{t,t+h})$  is estimated over three different horizons,  $h = 1, 3, 7$ .

$$\log(RV_{t,t+h}) = \alpha + \log(X_{RV}^\top) \beta_{RV} + \varepsilon_{t,t+h} \quad t = 1, 2, \dots, T, \tag{17}$$

where the explanatory variables vector is defined as

$$\log(X_{RV}^\top) = (\log(RV_D), \log(RV_W), \log(RV_M)),$$

which contains the multi-period lagged realized variance estimators defined previously. And the corresponding parameters vector is  $\beta_{RV} = (\beta_D, \beta_W, \beta_M)^\top$ . Based on the HAR model, one could construct a model that accounts jump components by simply adding the thresholded jump estimators which are discussed in section 2, thus we have

$$\log(RV_{t,t+h}) = \alpha + \log(X_{RV}^\top) \beta_{RV} + \log(X_J^\top) \beta_J + \varepsilon_{t,t+h} \quad t = 1, 2, \dots, T, \quad (18)$$

where the added jumps variables vector is

$$\log(X_J^\top) = (\log(J_D + 1), \log(J_W + 1), \log(J_M + 1)).$$

Note that here the logarithmic transform ensures that the jump estimators to be positive. And the corresponding parameters vector is  $\beta_J = (\beta_{JD}, \beta_{JW}, \beta_{JM})^\top$ . We abbreviate this model as **RVJ**. Furthermore, the HAR model can be decomposed with realized semi-variance estimators  $RSV^+$  and  $RSV^-$  which we name it as **RSV** model. Such that,

$$\log(RV_{t,t+h}) = \alpha + \log(X_{RSV}^\top) \beta_{RSV} + \varepsilon_{t,t+h} \quad t = 1, 2, \dots, T, \quad (19)$$

where the variables vector included positive/negative lagged regressors is defined as

$$\log(X_{RSV}^\top) = (\log(RSV_D^+), \log(RSV_W^+), \log(RSV_M^+), \log(RSV_D^-), \log(RSV_W^-), \log(RSV_M^-)).$$

Correspondingly, the parameters vector is  $\beta_{RSV} = (\beta_D^+, \beta_W^+, \beta_M^+, \beta_D^-, \beta_W^-, \beta_M^-)^\top$ . With analogous arguments, we can formulate the **RSVSJ** model by extending the RSV with positive/negative jumps, i.e

$$\log(RV_{t,t+h}) = \alpha + \log(X_{RSV}^\top) \beta_{RSV} + \log(X_{J+/-}^\top) \beta_{J+/-} + \varepsilon_{t,t+h} \quad t = 1, 2, \dots, T, \quad (20)$$

where the jump variables vector is

$$\log(X_{J+/-}^\top) = (\log(J_D^+ + 1), \log(J_W^+ + 1), \log(J_M^+ + 1), \log(J_D^- + 1), \log(J_W^- + 1), \log(J_M^- + 1)),$$

and the jumps coefficients vector is  $\beta_{J+/-} = (\beta_{JD}^+, \beta_{JW}^+, \beta_{JM}^+, \beta_{JD}^-, \beta_{JW}^-, \beta_{JM}^-)^\top$ .

All coefficients,  $\beta_{RV}$ ,  $\beta_J$ ,  $\beta_{RSV}$ , and  $\beta_{J+/-}$  are estimated by OLS. To adjust the possible serial correlation and heteroskedasticity of the error term, we use the Newey-West covariance matrix estimator with 7, 14 and 60 lags for daily, weekly and monthly forecast horizon, respectively. Note that all the jump estimators are based on  $\alpha = 0.9999$  and  $c_\theta = 3$ . To summarize it up, we construct 4 forecasting models in equations from (17)-(20) abbreviated as **HAR**, **RVJ**, **RSV**, **RSVSJ**.

#### 4.2. In-Sample Forecasting Analysis

To analyze how each explanatory variable affects future  $RV$ , we fit each of the forecasting models with full sample, i.e from the start of 2017 until the Middle of 2019<sup>14</sup>, named as full-sample forecasting.

Table 3 reports the regression results of HAR and RVJ models in which estimators are not decomposed into positive and negative. The in-sample forecasting results show consistently that the lagged  $RV$  has a strong and persistent positive relationship with future  $RV$  in all of the three forecasting horizons. For example, the coefficient of 1-day lagged  $\log(RV)$  can be up to 0.600. The significance of autocorrelation decays as the estimator lagged more, e.g  $\beta_D = 0.568$  and  $\beta_W = 0.236$  for HAR model in  $h = 1$  case as shown in BTC-D part of table 3. And this effect decays with longer forecasting horizon, e.g  $\beta_D = 0.568$  in  $h = 1$  case, and  $\beta_D = 0.202$  in  $h = 30$  case. Also, the 1-day lagged detected jumps induce significant lower future realized variances in both BTC-D and BTC-G across all of the three forecasting horizons. This suggests that higher jump shocks, on average, actually reduce future risk. Further more, the Adj- $R^2$  raises along with the forecasting horizon, e.g in BTC-D from 0.333 in  $h = 1$  case to 0.397 in  $h = 30$  case.

Table 4 contains the in-sample forecasting results of RSV and RSVSJ model which account for the positive and negative effect from past realized variances or jumps. It shows that future realized variances of BTC is strongly impacted by the positive jumps, and such impact is significant and persistent. One can see that there is a significant negative relationship between the positive jumps and future realized variances in those three forecasting horizons. While the relationships in most cases between negative jumps and future realized variances are insignificant. This finding slightly differs from the result in Patton and Sheppard (2015) in which negative jumps lead to significant higher future volatility. Also, one can see that both the positive and negative realized variances lead to significant higher future realized variances.

One of the assumptions of the full-sample forecasting is the stability of coefficients, namely

---

<sup>14</sup>The sample date lasts until July 2019 for BTC-D and May 2019 for BTC-G

**Table 3:** Full-Sample Fitting Regression Results of Unsigned Estimators

**HAR:**  $\log(RV_{t,t+h}) = \alpha + \log(X_{RV}^\top) \beta_{RV} + \varepsilon_{t,t+h}$       **RVJ:**  $\log(RV_{t,t+h}) = \alpha + \log(X_{RV}^\top) \beta_{RV} + \log(X_J^\top) \beta_J + \varepsilon_{t,t+h}$   
 Regressors vectors:  $\log(X_{RV}^\top) = (\log(RV_D), \log(RV_W), \log(RV_M))$ , and  $\log(X_J^\top) = (\log(J_D + 1), \log(J_W + 1), \log(J_M + 1))$   
 Parameters vectors:  $\beta_{RV} = (\beta_D, \beta_W, \beta_M)^\top$ , and  $\beta_J = (\beta_{JD}, \beta_{JW}, \beta_{JM})^\top$

|             | BTC-D             |                  |                  |                    |                    |                    | M-Z R <sup>2</sup> | BTC-G             |                  |                  |                    |                    |                    | M-Z R <sup>2</sup> |
|-------------|-------------------|------------------|------------------|--------------------|--------------------|--------------------|--------------------|-------------------|------------------|------------------|--------------------|--------------------|--------------------|--------------------|
|             | $\beta_D$         | $\beta_W$        | $\beta_M$        | $\beta_{JD}$       | $\beta_{JW}$       | $\beta_{JM}$       |                    | $\beta_D$         | $\beta_W$        | $\beta_M$        | $\beta_{JD}$       | $\beta_{JW}$       | $\beta_{JM}$       |                    |
| <b>h=1</b>  |                   |                  |                  |                    |                    |                    |                    |                   |                  |                  |                    |                    |                    |                    |
| HAR         | 0.568<br>(15.758) | 0.236<br>(5.387) | 0.132<br>(2.797) |                    |                    |                    | 0.333              | 0.532<br>(16.773) | 0.262<br>(6.793) | 0.127<br>(2.856) |                    |                    |                    | 0.255              |
| RVJ         | 0.600<br>(17.108) | 0.225<br>(4.745) | 0.096<br>(2.164) | -0.574<br>(-3.053) | -0.534<br>(-1.932) | -0.489<br>(-1.350) | 0.330              | 0.550<br>(16.423) | 0.313<br>(7.01)  | 0.071<br>(1.525) | -0.412<br>(-2.452) | -0.643<br>(-3.275) | -0.232<br>(-0.835) | 0.248              |
| <b>h=7</b>  |                   |                  |                  |                    |                    |                    |                    |                   |                  |                  |                    |                    |                    |                    |
| HAR         | 0.374<br>(9.679)  | 0.209<br>(3.199) | 0.248<br>(2.439) |                    |                    |                    | 0.348              | 0.342<br>(8.917)  | 0.208<br>(3.473) | 0.203<br>(2.556) |                    |                    |                    | 0.319              |
| RVJ         | 0.417<br>(10.367) | 0.175<br>(2.435) | 0.21<br>(2.13)   | -0.811<br>(-4.258) | -0.684<br>(-1.078) | -2.057<br>(-2.426) | 0.327              | 0.393<br>(9.605)  | 0.158<br>(2.405) | 0.233<br>(2.819) | -0.605<br>(-3.791) | 0.019<br>(0.049)   | -1.312<br>(-2.48)  | 0.323              |
| <b>h=30</b> |                   |                  |                  |                    |                    |                    |                    |                   |                  |                  |                    |                    |                    |                    |
| HAR         | 0.202<br>(5.199)  | 0.15<br>(1.885)  | 0.312<br>(2.783) |                    |                    |                    | 0.397              | 0.154<br>(5.046)  | 0.149<br>(2.642) | 0.228<br>(1.703) |                    |                    |                    | 0.417              |
| RVJ         | 0.222<br>(6.117)  | 0.125<br>(1.519) | 0.268<br>(2.602) | -0.750<br>(-3.343) | -1.237<br>(-1.833) | -4.386<br>(-4.972) | 0.366              | 0.155<br>(4.831)  | 0.138<br>(2.201) | 0.293<br>(2.934) | -0.340<br>(-2.015) | -0.402<br>(-1.121) | -2.366<br>(-5.339) | 0.416              |

The table contains results for BTC-D (left-hand side part) and BTC-G (right-hand side part). Each of the panel of the two parts reports the regression results of HAR and RVJ models. Panels from top to bottom are realized variance forecasts in three different horizons,  $h = 1, 7, 30$ . The first six columns of each panel show the coefficients and the last column is the Adj-R<sup>2</sup>. The  $t$ -value is in the parenthesis. All parameters are estimated by OLS using Newey-West covariance matrix estimator with 7, 14 and 60 lags for  $h = 1, 7, 30$ , respectively.

**Table 4:** Full-Sample Fitting Regression Results of Signed Estimators

**RSV:**  $\log(RV_{t,t+h}) = \alpha + \log(X_{RSV}^\top) \beta_{RSV} + \varepsilon_{t,t+h}$       **RSVSJ:**  $\log(RV_{t,t+h}) = \alpha + \log(X_{RSV}^\top) \beta_{RSV} + \log(X_{J+-}^\top) \beta_{J+-} + \varepsilon_{t,t+h}$   
 Regressors vectors  $\log(X_{RSV}^\top) = (\log(RSV_D^+), \log(RSV_W^+), \log(RSV_M^+), \log(RSV_D^-), \log(RSV_W^-), \log(RSV_M^-))$ ,  
 and  $\log(X_{J+-}^\top) = (\log(J_D^+ + 1), \log(J_W^+ + 1), \log(J_M^+ + 1), \log(J_D^- + 1), \log(J_W^- + 1), \log(J_M^- + 1))$   
 Parameters vectors:  $\beta_{RSV} = (\beta_D^+, \beta_W^+, \beta_M^+, \beta_D^-, \beta_W^-, \beta_M^-)^\top$ , and  $\beta_{J+-} = (\beta_{JD}^+, \beta_{JW}^+, \beta_{JM}^+, \beta_{JD}^-, \beta_{JW}^-, \beta_{JM}^-)^\top$

|             | BTC-D           |                 |                 |                    |                    |                    |                    | BTC-G           |                 |                 |                    |                    |                    |                    |
|-------------|-----------------|-----------------|-----------------|--------------------|--------------------|--------------------|--------------------|-----------------|-----------------|-----------------|--------------------|--------------------|--------------------|--------------------|
|             | $\beta_D^{+/-}$ | $\beta_W^{+/-}$ | $\beta_M^{+/-}$ | $\beta_{JD}^{+/-}$ | $\beta_{JW}^{+/-}$ | $\beta_{JM}^{+/-}$ | M-Z R <sup>2</sup> | $\beta_D^{+/-}$ | $\beta_W^{+/-}$ | $\beta_M^{+/-}$ | $\beta_{JD}^{+/-}$ | $\beta_{JW}^{+/-}$ | $\beta_{JM}^{+/-}$ | M-Z R <sup>2</sup> |
| <b>h=1</b>  |                 |                 |                 |                    |                    |                    |                    |                 |                 |                 |                    |                    |                    |                    |
| RSV         | 0.202           | 0.045           | 0.069           |                    |                    |                    | 0.339              | 0.238           | 0.103           | 0.235           |                    |                    |                    | 0.259              |
|             | (2.999)         | (0.434)         | (0.519)         |                    |                    |                    |                    | (4.129)         | (1.032)         | (2.205)         |                    |                    |                    |                    |
|             | 0.375           | 0.182           | 0.057           |                    |                    |                    |                    | 0.303           | 0.146           | -0.109          |                    |                    |                    |                    |
|             | (5.939)         | (1.719)         | (0.421)         |                    |                    |                    |                    | (5.47)          | (1.566)         | (-0.98)         |                    |                    |                    |                    |
| RSVSJ       | 0.255           | 0.212           | -0.005          | -0.454             | -1.367             | 0.542              | 0.360              | 0.317           | 0.259           | 0.150           | -0.689             | -1.799             | -0.710             | 0.299              |
|             | (3.299)         | (1.713)         | (-0.029)        | (-2.164)           | (-3.09)            | (0.755)            |                    | (4.115)         | (1.883)         | (0.715)         | (-2.241)           | (-3.397)           | (-0.689)           |                    |
|             | 0.353           | 0.079           | 0.104           | -0.264             | -0.178             | -0.586             |                    | 0.247           | 0.100           | -0.044          | -0.060             | -0.152             | -0.228             |                    |
|             | (4.557)         | (0.624)         | (0.54)          | (-1.106)           | (-0.363)           | (-0.746)           |                    | (3.271)         | (0.840)         | (-0.213)        | (-0.258)           | (-0.557)           | (-0.385)           |                    |
| <b>h=7</b>  |                 |                 |                 |                    |                    |                    |                    |                 |                 |                 |                    |                    |                    |                    |
| RSV         | 0.156           | 0.012           | 0.273           |                    |                    |                    | 0.351              | 0.170           | 0.122           | 0.368           |                    |                    |                    | 0.323              |
|             | (2.463)         | (0.058)         | (0.892)         |                    |                    |                    |                    | (2.944)         | (0.671)         | (1.311)         |                    |                    |                    |                    |
|             | 0.230           | 0.192           | -0.033          |                    |                    |                    |                    | 0.18            | 0.077           | -0.165          |                    |                    |                    |                    |
|             | (3.972)         | (0.935)         | (-0.1)          |                    |                    |                    |                    | (3.226)         | (0.453)         | (-0.574)        |                    |                    |                    |                    |
| RSVSJ       | 0.293           | 0.386           | 0.341           | -0.989             | -2.345             | -0.825             | 0.362              | 0.340           | 0.389           | 0.354           | -1.246             | -1.998             | -3.376             | 0.381              |
|             | (4.456)         | (1.632)         | (0.785)         | (-4.011)           | (-2.672)           | (-0.581)           |                    | (4.667)         | (1.544)         | (0.707)         | (-4.516)           | (-2.492)           | (-1.74)            |                    |
|             | 0.169           | -0.141          | -0.071          | -0.456             | 0.474              | -1.101             |                    | 0.086           | -0.196          | 0.001           | -0.088             | 0.929              | -0.977             |                    |
|             | (2.544)         | (-0.57)         | (-0.153)        | (-2.001)           | (0.443)            | (-0.536)           |                    | (1.164)         | (-0.876)        | (0.003)         | (-0.43)            | (1.673)            | (-0.815)           |                    |
| <b>h=30</b> |                 |                 |                 |                    |                    |                    |                    |                 |                 |                 |                    |                    |                    |                    |
| RSV         | 0.093           | 0.033           | 0.489           |                    |                    |                    | 0.402              | 0.082           | 0.039           | 0.348           |                    |                    |                    | 0.430              |
|             | (1.234)         | (0.134)         | (0.916)         |                    |                    |                    |                    | (1.498)         | (0.27)          | (1.014)         |                    |                    |                    |                    |
|             | 0.122           | 0.121           | -0.191          |                    |                    |                    |                    | 0.08            | 0.101           | -0.117          |                    |                    |                    |                    |
|             | (2.362)         | (0.518)         | (-0.334)        |                    |                    |                    |                    | (1.947)         | (0.731)         | (-0.305)        |                    |                    |                    |                    |
| RSVSJ       | 0.195           | 0.272           | 0.583           | -0.743             | -1.52              | -2.978             | 0.388              | 0.185           | 0.239           | -0.095          | -0.77              | -2.039             | -3.162             | 0.469              |
|             | (3.493)         | (1.252)         | (0.659)         | (-3.533)           | (-2.422)           | (-1.514)           |                    | (3.199)         | (1.664)         | (-0.162)        | (-4.088)           | (-3.769)           | (-1.28)            |                    |
|             | 0.07            | -0.101          | -0.071          | -0.354             | -0.095             | -3.716             |                    | -0.011          | -0.046          | 0.579           | 0.098              | 0.336              | -3.214             |                    |
|             | (1.648)         | (-0.464)        | (-0.075)        | (-1.213)           | (-0.112)           | (-1.281)           |                    | (-0.313)        | (-0.347)        | (1.012)         | (0.668)            | (1.107)            | (-2.193)           |                    |

The table contains results for BTC-D (left-hand side part) and BTC-G (right-hand side part). Each of the panel of the two parts reports the regression results of RSV and RSVSJ models. Panels from top to bottom are realized variance forecasts in three different horizons,  $h = 1, 7, 30$ . The first six columns of each panel show the coefficients and the last column is the Adj-R<sup>2</sup>. Each regression model of the three panels is separated by line in which upper (bottom) part reports the results of the positive (negative) signed estimators. The  $t$ -value is in the parenthesis. All parameters are estimated by OLS using Newey-West covariance matrix estimator with 7, 14 and 60 lags for  $h = 1, 7, 30$ , respectively.

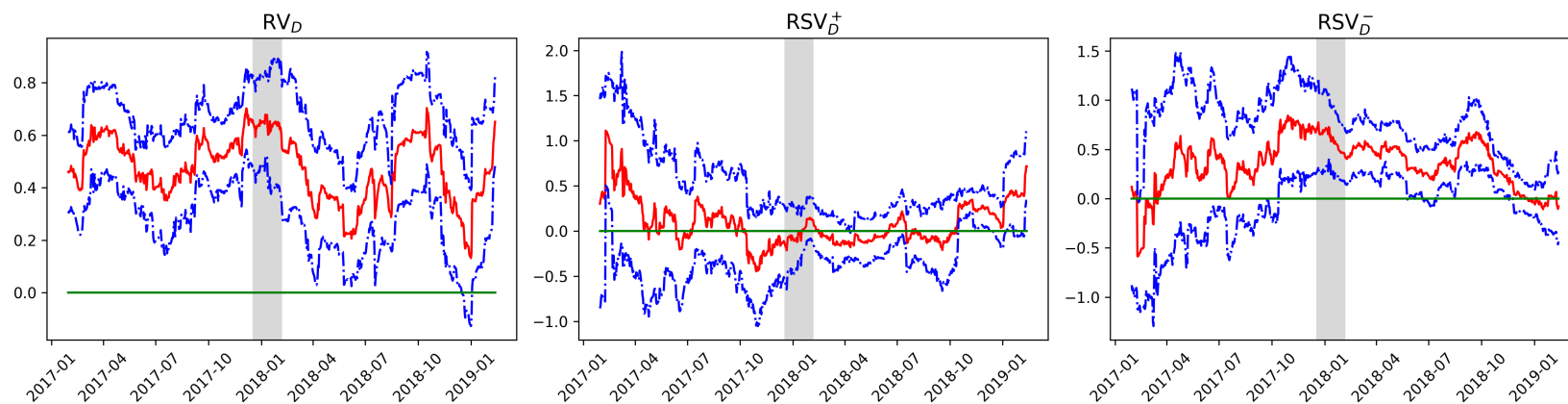
the market is not changing too volatile. However, such an assumption is too strong for the Bitcoin market in which a lot of speculations have been happening. When the market changes intensively, any model could be biased if it is calibrated only in a certain period. Hence, such a fitted model would underperform in the out-of-sample forecasting as the forecasting period could deviate from the fitting period substantially. We implement the rolling window method to allow the parameters changing over time, then the more reasonable comparisons can be obtained.

The adaptive method mimics an investor who updates the forecasting model based on the most recent information. A simple case is assuming that such updates are based on a fixed amount of lagged information. The window size  $T$  of the adaptive HAR models employed here is 90-days, i.e models are estimated by using past 90-days samples. And all the models are re-estimated every day. After the re-estimation of each day, the out-of-sample forecasts are performed in horizons  $h = 1, 7, 30$ , spontaneously. As a result, we re-estimate each model 744-times for BTC-D and 763-times for BTC-G.

Fig. 5 shows the changing of parameters  $\beta_D^{+/-}$  of the unsigned and signed one-day estimator in HAR and RSV model. The parameters are evolving systematically which justify the adaptive forecasting method. The red solid lines represent the point estimation of parameters, the blue lines are the confidence interval with a 95% confidence level, and the green horizontal line indicates the zero value. The left figure of each panel confirms that the significant positive impact of 1-day lagged  $RV$  is persistent during the whole sample. The other two figures show the upside and downside risk estimators play "complementary" roles in forecasting over time. Over the 2 years, the upside risk coefficients  $\beta_D^+$  evolve as a u-shape curve, and oppositely the pattern of the downside risk coefficients  $\beta_D^-$  are similar to an inverse u-shape curve. Despite the full-sample fitting suggesting that both upside risk and downside risk lead to higher future realized variances, one can see that the coefficient of downside risk  $RSV_D^-$  tends to be positive in the whole sample, and significant in a long period. Fig. 6 contains the evolving of the parameter of one-day lagged estimator, i.e  $\beta_{JD}$  in RVJ and  $\beta_{JD}^{+/-}$  RSVSJ model. The left figure of each panel suggests that jumps will lead to a significant higher future realized variances. The right two figures show that the parameters of signed jump estimators are fluctuating below zero most of the time, which indicates the negative (insignificant) impact of signed jumps. Comparing with the negative jumps, the positive jumps  $J^+$  have a more consistent negative relationship between future realized variances.

One of the most interesting periods of BTC is the huge market crash at the beginning of 2018. We mark the period from December 27th, 2017 (peak price day) to February 6th, 2018 (the lowest point in this crash) with grey shadow in Fig. 5 and 6. Both the parameters  $\beta_D$

(a) BTC-D Coefficients and  $t$ -values of evolving. From Feb. 2017 to Feb. 2019



(b) BTC-G Coefficients and  $t$ -values of evolving. From Feb. 2017 to Apr. 2019

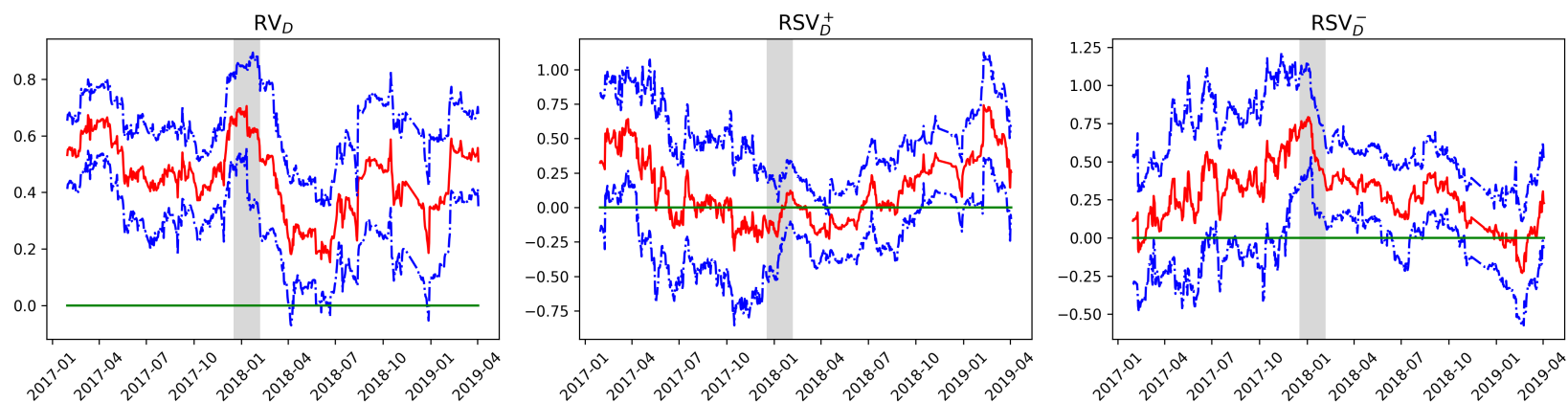
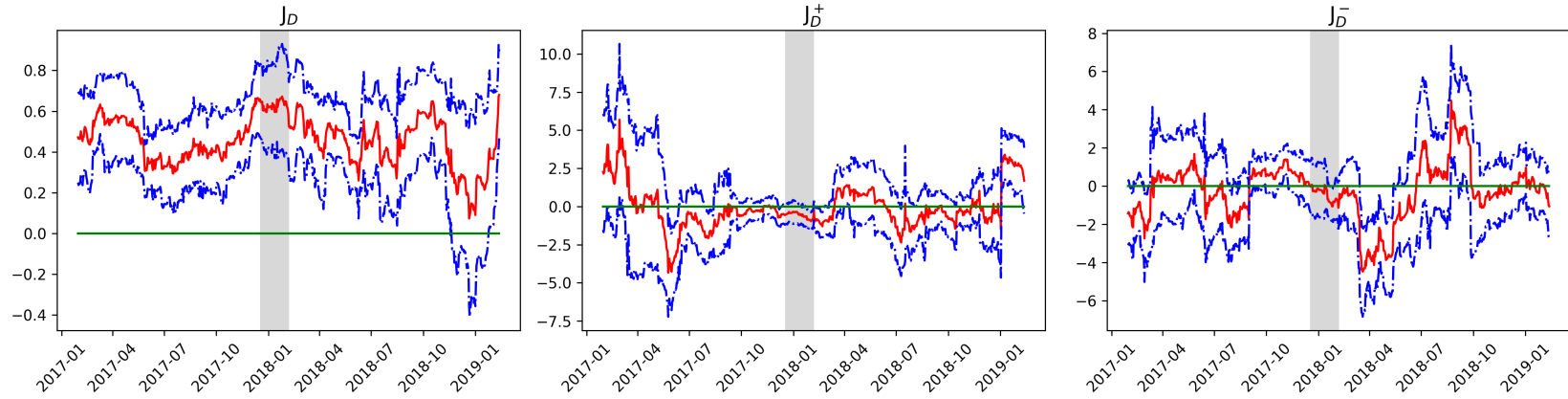


**Fig. 5:** Point estimation of parameter (solid red line) and the confidence interval with 95% confidence level (blue dash line) change over time. Panel (a) reports BTC-D case from Feb. 2017 to Feb. 2019 and panel (b) reports BTC-G case from Feb. 2017 to Apr. 2019. For each panel, figures from left to right are coefficients of  $RV_D$  from HAR model,  $RSV_D^+$  and  $RSV_D^-$  from RSV model, respectively. The green horizontal line represents the value of zero and vertical grey band marks the period from Dec. 17th 2017 to Feb. 6th 2018.

(a) BTC-D Coefficients and  $t$ -values of evolving. From Feb. 2017 to Feb. 2019



(b) BTC-G Coefficients and  $t$ -values of evolving. From Feb. 2017 to Apr. 2019

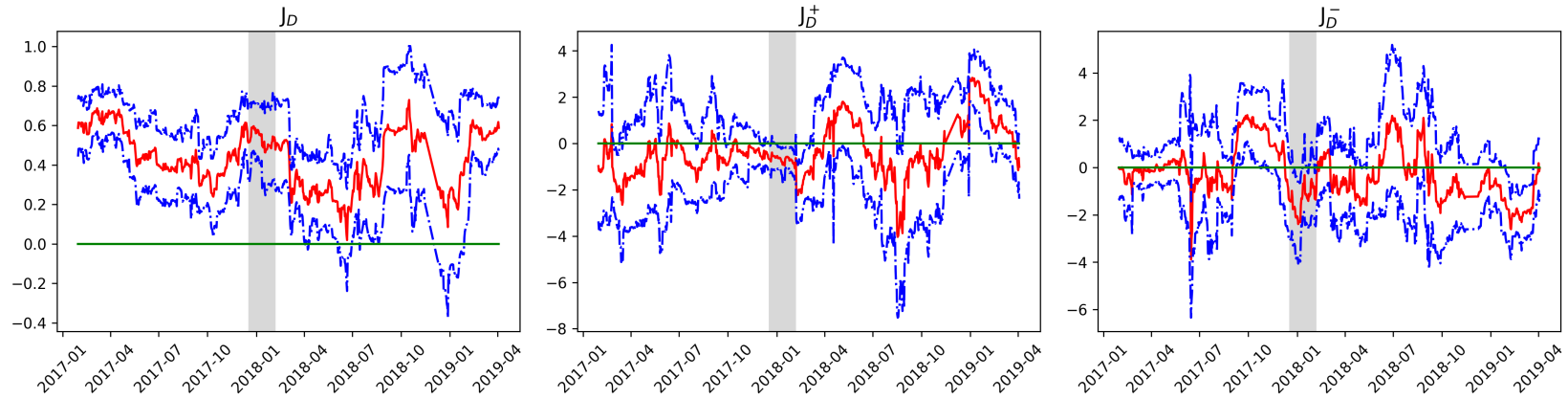


**Fig. 6:** Point estimation of parameter (solid red line) and the confidence interval with 95% confidence level (blue dash line) change over time. Panel (a) reports BTC-D case from Feb. 2017 to Feb. 2019 and panel (b) reports BTC-G case from Feb. 2017 to Apr. 2019. For each panel, figures from left to right are coefficients of  $J_D$  from RVJ model,  $J_D^+$  and  $J_D^-$  from RSVSJ model, respectively. The green horizontal line represents the value of zero and vertical grey band marks the period from Dec. 17th 2017 to Feb. 6th 2018.



and  $\beta_{JD}$  in both BTC-D and BTC-G (left figure of each panel in Fig. 5 and 6) reach a high level in this period which means that future realized variances are positively impacted by realized variances and jumps, significantly. More importantly, one can see that the negative realized variances and positive jumps lead to significant changes in future realized variances as shown in the right figures of Fig. 5 and 6. Specifically, the downside risk has a significant positive relationship with future risk, while the positive jumps bring lower future risk during this bearish market. The rationale behind this finding is that when the market is seen to be falling, on one hand, higher the downside risk more of the investors incline to escape, hence the market gets more volatile. On the other hand, the positive price jumps may create the illusion of market bouncing back which could calm down the market and decrease the volatility.

### 4.3. *Out-of-Sample Forecasts Evaluation*

In this subsection, we further discuss the out-of-sample forecasting results aiming for comparing different models. All the out-of-sample forecasts are computed using 90-days rolling-window HAR regressions as described in the previous sections. Parameters are re-estimated on a daily basis. Here the "insanity filter" is applied in which we ensure that any forecast is no smaller (larger) than the minimum (maximum) realization of the past (Patton and Sheppard (2015), Swanson and White (1997) and Bollerslev et al. (2018)).

#### 4.3.1. *Forecasting Accuracy*

The out-of-sample performance evaluations are based on the squared form, i.e results from the log-log forecasting models are transformed back to squared form for a fair comparison<sup>15</sup>. We employ four metrics for the forecasting performance comparison. The first one is  $R^2$  from Mincer-Zarnowitz forecasting regression, named  $MZ-R^2$ . The following three metrics named MSE, HRMSE, and QLIKE are computed from corresponding loss functions,

---

<sup>15</sup>The squared form of HAR models are also common in previous literature, and usually underperforms the logarithmic form. We also report the squared form forecasting accuracy in Appendix 8, the conclusions are consistent with logarithmic form

$$L^{\text{MSE}} = \left( RV_{t,t+h} - \widehat{RV}_{t,t+h} \right)^2 \quad (21)$$

$$L^{\text{HRMSE}} = \left( \frac{RV_{t,t+h} - \widehat{RV}_{t,t+h}}{RV_{t,t+h}} \right)^2 \quad (22)$$

$$L^{\text{QLIKE}} = \log \widehat{RV}_{t,t+h} + \frac{RV_{t,t+h}}{\widehat{RV}_{t,t+h}}, \quad (23)$$

where  $\widehat{RV}_{t,t+h}$  is the forecast average realized variance over time period  $[t, t+h]$ , and  $RV_{t,t+h}$  is the corresponding true value. And then the D-M test (Diebold and Mariano (2002)) is used to test the significance of comparison results by embedding the three loss functions. The mean squared error (MSE) is the mean value of quadratic loss function  $L^{\text{MSE}}$  which measures the Euclidean distance between the ex-post realized variance and forecast result. The heteroscedasticity adjusted root mean squared error (HRMSE) defined as the squared root mean of  $L^{\text{HRMSE}}$  (Bollerslev and Ghysels (1996)) is a more robust metric to the scale changing of realized variance. The third metric QLIKE is the mean of a gaussian quasi-likelihood loss function  $L^{\text{QLIKE}}$  (Patton (2011)) which gives consistent evaluation on different imperfect volatility proxies.

The out-of-sample forecasting evaluation reported in Tab.5 shows clearly that the forecasting performance depends on the forecasting horizon. This conclusion has a twofold meaning. First of all, it is obvious that each of the models performs better in the long forecasting horizon under most of the metrics, such as the  $MZ-R^2$  is higher and MSE is much lower in  $h = 30$ . Secondly, it partially reveals the necessity of modeling jumps or decomposition into signed estimators. In the short forecasting horizon,  $h = 1$ , those models that do not put jump components as explanatory variables separately, HAR and RSV models, tend to outperform any other models. For example,  $MZ-R^2$  is 0.299 in HAR while it is 0.241 in RSVSJ which accounts for the decomposed estimators  $SRV$  and  $J^{+/-}$ . As shown in the first panel of Table 5, the D-M test shows the better accuracy of HAR at 5% significant level. However, in the long forecasting horizon case,  $h = 30$ , modeling the jumps and signed estimators does improve the forecasting performance. As shown in the last panel of Table 5, the models accounting jumps or signed estimators including RVJ, RSV, and RSVSJ, outperform HAR model by all the metrics. And the significance is confirmed by the D-M test at the 5% significant level. Contrary to Andersen et al. (2007), we find evidence that modeling separated jumps or signed estimators do not necessarily improve the BTC  $RV$  forecasting accuracy and forecasting horizon matters. However, the theoretical explanation of that is not answered as far as we know.

**Table 5:** Adaptive Log-Log HAR Models Out-of-Sample Forecasts Performance Evaluation

|                   | BTC-D |                    |                    |                    | BTC-G |                    |        |                    |
|-------------------|-------|--------------------|--------------------|--------------------|-------|--------------------|--------|--------------------|
|                   | HAR   | RVJ                | RSV                | RSVSJ              | HAR   | RVJ                | RSV    | RSVSJ              |
| <b>h=1</b>        |       |                    |                    |                    |       |                    |        |                    |
| MZ-R <sup>2</sup> | 0.299 | 0.287              | 0.289              | 0.241              | 0.261 | 0.218              | 0.266  | 0.235              |
| MSE               | 3.260 | 3.356              | 3.313              | 3.680              | 2.217 | 2.353              | 2.209  | 2.298              |
| HRMSE             | 0.760 | 0.822 <sup>†</sup> | 0.807 <sup>†</sup> | 0.937 <sup>†</sup> | 0.979 | 1.004              | 0.985  | 1.143              |
| QLIKE             | 0.902 | 0.972              | 0.920              | 1.085 <sup>†</sup> | 0.906 | 1.017              | 0.945  | 1.170 <sup>†</sup> |
| <b>h=7</b>        |       |                    |                    |                    |       |                    |        |                    |
| MZ-R <sup>2</sup> | 0.327 | 0.366              | 0.333              | 0.392              | 0.329 | 0.277              | 0.352  | 0.406              |
| MSE               | 1.576 | 1.514              | 1.691              | 1.588              | 0.949 | 1.016              | 0.955  | 0.931              |
| HRMSE             | 0.881 | 0.903              | 1.091 <sup>†</sup> | 0.969              | 0.908 | 0.989 <sup>†</sup> | 0.888  | 0.971              |
| QLIKE             | 0.946 | 0.947              | 0.946              | 0.930              | 0.906 | 1.001 <sup>†</sup> | 0.929  | 0.978              |
| <b>h=30</b>       |       |                    |                    |                    |       |                    |        |                    |
| MZ-R <sup>2</sup> | 0.504 | 0.680              | 0.569              | 0.604              | 0.591 | 0.635              | 0.632  | 0.708              |
| MSE               | 0.729 | 0.488*             | 0.611*             | 0.584*             | 0.348 | 0.305*             | 0.307* | 0.247*             |
| HRMSE             | 0.628 | 0.488*             | 0.543*             | 0.451*             | 0.582 | 0.549*             | 0.509* | 0.384*             |
| QLIKE             | 0.965 | 0.910*             | 0.885*             | 0.878*             | 0.773 | 0.746*             | 0.744* | 0.725*             |

The table reports the out-of-sample forecasting performance of BTC-D (left part) and BTC-D (right part) in different forecasting horizons  $h = 1, 7, 30$  separated into three panels. The columns of each panel from left to right are HAR, RVJ, RSV, and RSVSJ models detailed in section 4.1. The rows of each panel from top to down are R<sup>2</sup> of Mincer-Zarnowitz forecasting regression, mean squared error, heteroscedasticity adjusted root mean squared error, and mean of gaussian quasi-likelihood error. The † marks when the HAR model outperforms significantly other models, while the \* denotes that the HAR model underperforms other models significantly, and the significance is confirmed by D-M test at 5% significant level. The forecasts are conducted in logarithmic forms, and then transformed by to squared form for the performance evaluation.

#### 4.3.2. Economic Value

It is a stylized fact that the model performance evaluation is heavily influenced by the choice of metrics. For example, in the case of BTC-G  $h = 1$  shown in Table 5, the HAR model underperforms RSV by MZ-R<sup>2</sup>, however, one can find that HAR has smaller forecasting errors than that of RSV by both HRMSE and QLIKE.

As the validity of forecasting realized variance is to be tested by the market, we employ the approach of Bollerslev et al. (2018). The advantages of this approach relative to the framework of Fleming et al. (2001) are twofold. This so-called RU-framework evaluates utility without requiring forecasts on asset returns. Then, it mimics a trading strategy when an investor targets at a constant Sharp ratio and adjust his/her risky asset positions according to the  $RV$  forecasts. A first-order expansion on expected utility yields (for  $h = 1$ )

$$E[u(W_{t+1})] = E(W_{t+1}) - \frac{1}{2}\gamma^A V(W_{t+1}), \quad (24)$$

where  $\gamma^A$  is the absolute Pratt-Arrow risk aversion. The Realized Utility  $RU_{t+1}^{(m)}$  at time

$t + 1$  by model  $m$  defined as utility per wealth with optimal weights  $\text{RU}_{t+1}^{(m)} = \text{EU}(\omega_t^{(m)})/W_t$  is given by (See Appendix B.3 for more details of realized utility):

$$\text{RU}_{t+1}^{(m)} = \frac{SR^2}{\gamma} \left( \sqrt{\frac{RV_{t+1}}{\widehat{RV}_{t+1}^{(m)}}} - \frac{1}{2} \frac{RV_{t+1}}{\widehat{RV}_{t+1}^{(m)}} \right), \quad (25)$$

where  $RV_{t+1}$  and  $\widehat{RV}_{t+1}$  are the ex-post and forecast realized variance of  $t + 1$ . Sharp ratio  $SR = 0.4$  and relative risk aversion  $\gamma = 2$  are given as constant. If one has perfect forecast, i.e  $\widehat{RV}_{t+1}^{(m)} = RV_{t+1}$ , then  $\text{RU}_{t+1}^{(m)} = \frac{SR^2}{2\gamma} = 4\%$ .

As the optimal weight is given by (35) in Appendix B.3, for an investor given constant  $SR/\gamma$ , lower risk the investor expects for the next day, higher the proportion of wealth should be allocated to risky asset. And in the case that  $\sqrt{\widehat{RV}_{t+1}^{(m)}} < SR/\gamma$ , then  $\omega_t^{(m)} > 1$  implies a leverage investment. However, we restrict the weight as  $\omega_t \in [0, 1]$ . Consequently, when  $\omega_t^{(m)} > 1$ , the realized utility  $\text{RU}_t^{(m)} = SR \cdot \sqrt{RV_{t+1}} - \frac{\gamma}{2}RV_{t+1}$  which is the case when  $\omega_t^{(m)} = 1$ .

$$\text{RU}_{t+1}^{(m)} = \begin{cases} \frac{SR^2}{\gamma} \left( \sqrt{\frac{RV_{t+1}}{\widehat{RV}_{t+1}^{(m)}}} - \frac{1}{2} \frac{RV_{t+1}}{\widehat{RV}_{t+1}^{(m)}} \right), & \frac{SR}{\gamma} \leq \sqrt{\widehat{RV}_{t+1}^{(m)}} \\ SR \cdot \sqrt{RV_{t+1}} - \frac{\gamma}{2}RV_{t+1}, & \text{otherwise} \end{cases} \quad (26)$$

Clearly, the comparison almost solely depends on the forecasts  $\widehat{RV}_{t+1}^{(m)}$  illustrated in (26). Note that each of the forecasting models is in logarithmic form, the realized utility is calculated after transforming the logarithmic forecast to squared form. We also report the realized utility by squared form forecasting models in Appendix A.3.

By averaging the  $\text{RU}_{t+h}^{(m)}$  over time  $t \in [1, T]$ , one can have the realized utility  $\text{RU}^{(m)}$  for each model  $m$  on forecasting horizon  $h$ . The realized utility provides another metric to compare forecasts from different models. As explained above, better the forecast is, closer the  $\text{RU}_{t+h}^{(m)}$  to 4%.

$$\text{RU}_h^{(m)} = \frac{1}{T} \sum_{t=1}^T \text{RU}_{t+h}^{(m)} \quad (27)$$

The economic value reported in Table 6 confirms the conclusion from the out-of-sample forecasting. Firstly, an investor can gain higher utility regardless of the choice of the model if one forecasts in the long horizon risk. For example, the RSVSJ model gives around 227 basis points more utility in the case of  $h = 30$  than that of  $h = 1$  for BTC-D. Secondly, in the short horizon forecasting,  $h = 1$ , the HAR model provides much more utility than the other models do, for example, HAR outperforms RVJ by up to around 22 basis points which

**Table 6:** Economic Values Evaluation of Log-Log Models Out-of-Sample Forecasts (%)

|             | BTC-D        |       |              |              | BTC-G        |       |       |              |
|-------------|--------------|-------|--------------|--------------|--------------|-------|-------|--------------|
|             | HAR          | RVJ   | RSV          | RSVSJ        | HAR          | RVJ   | RSV   | RSVSJ        |
| <b>h=1</b>  | <b>2.619</b> | 2.404 | 2.583        | 2.146        | <b>2.098</b> | 1.728 | 2.019 | 1.393        |
| <b>h=7</b>  | 3.133        | 3.128 | 3.140        | <b>3.143</b> | <b>2.793</b> | 2.549 | 2.710 | 2.631        |
| <b>h=30</b> | 3.479        | 3.591 | <b>3.671</b> | 3.665        | 3.576        | 3.633 | 3.635 | <b>3.662</b> |

The table reports the economic value gained in terms of realized utility of BTC-D (left part) and BTC-G (right part). The columns of each part from left to right are realized utility from four different models including HAR, RVJ, RSV, and RSVSJ model detailed in section 4.1. Each of the forecasting models is in logarithmic form, and then the realized utility is calculated after transforming forecasts to squared form. The rows are realized utility in three different forecasting horizons,  $h = 1, 7, 30$ . The highest utility of each forecasting horizon is bolded for both BTC-D and BTC-G. All the realized utility are reported in percentage.

suggest that modeling realized variance with the jump in the short horizon risk forecasting case would not add economic values. However, in the longer horizon forecasting case,  $h = 30$ , accounting either jumps or signed estimators do provide extra utility, such as RVJ model outperforms HAR model by 11 basis points utility, and RSV outperforms HAR by around 19 basis points utility for BTC-D. This finding sheds light on realized variance forecasting models selection for BTC investors. BTC Investors who target at a certain risk level should select the forecasting model based on their investment horizons. Last but not least, the investors can gain more utility by investing in BTC-D than on BTC-G in the short horizon forecasting case. BTC-D is a simple equal-weighted price portfolio which diversifies exchange idiosyncratic discontinuities changes risk (jumps) on price. While BTC-G suffers from the extra risk inherent in some specific exchanges.

## 5. Conclusion

This paper studies the risk of the Bitcoin market based on two high-frequency intraday data sources BTC-D and BTC-G for the sample period from January 2017 to Mid-2019. We first separate the risk sources of BTC in volatility and jumps employing the jump component separation method discussed in Barndorff-Nielsen and Shephard (2004) Barndorff-Nielsen and Shephard (2006) and Andersen et al. (2007). Unfortunately, this separation method fails to display some of the obvious jumps on the BTC price process caused by consecutive jumps. We correct the bias and separate the jump estimator  $J$  by employing the thresholded jump method (Corsi et al. (2010)). Further more, to disentangle the positive and negative risk,  $RV$  is further decomposed into positive estimators including upside risk  $RSV^+$ , positive jump  $J^+$ , and negative estimators including downside risk  $RSV^-$ , negative jump  $J^-$  (Barndorff-Nielsen et al. (2008b), Patton and Sheppard (2015)). Then, the empirical study is conveyed

in two parts. The first part reports the risk characteristics of BTC and the second part discusses the forecasting of BTC realized variance using different models.

The high risk of BTC can be observed by its high realized variance and jumps. The realized variance of BTC is much higher than any of the other traditional assets, and more than 40% of the days in the sample are identified with jumps. Surprisingly, despite the jumps being detected frequently, the discontinuities do not contribute much to the risk compared with the continuous path. During our sample period, the number of positive jumps approximately equals the number of negative jumps suggesting that a jump is not necessary a crash event. Such finding is contrary to the empirical results in Scaillet et al. (2018) concluding that most jumps in BTC are positive from June 2011 to November 2013. Lastly, we find that the idiosyncratic jump risk can be significantly reduced by a simple 3-exchange equal-weighted portfolio, BTC-D. This result implies that investors should at least diversify their BTC investment into different exchanges for lower jump risk.

In the second part of the empirical study, we focus on answering two questions:

1. How are the different estimators impact future realized variance of BTC?
2. Are modeling jumps and signed estimators explicitly in BTC necessary to improve forecasting accuracy and provide extra economic value?

Four log-log form forecasting models motivated by HAR (Corsi (2009)) are developed to investigate how lagged realized variance, jumps and signed estimators impact  $RV_{t+h}$ ,  $h = 1, 7, 30$ . We first conduct a full in-sample regression and then proceed with a 90-day rolling window out-of-sample forecast in which parameters update on a daily basis. The in-sample evidence suggests that future realized variance has a positive relationship between the downside risk  $RSV_D^-$  and the negative relationship between the positive jump  $J_D^+$ . And the one-day lagged unsigned jump leads significant lower realized variance. After allowing the parameters to be adaptive, we can observe that the parameters are changing systematically. Those effects stated above appear to be significant during the BTC market crash from the end of December 2017 to the start of February 2018.

Later in the out-of-sample forecasting subsection, we find that the performance evaluation of a forecasting model heavily depends on the forecasting horizon  $h$ . First, each of the models performs better in the long forecasting horizon in most of the performance metrics. More crucially, the forecasting horizon plays an important role in selecting a forecasting model. In the short horizon forecasting,  $h = 1$ , both adding jump components to the basic HAR model and decomposing  $RV$  into  $RSV$  reduce forecasting accuracy significantly. However, in the case of  $h = 30$ , the separation and decomposition models will outperform HAR significantly. This is likely caused by the overreaction on jumps from models, but the

theoretical explanation needs to be further established. Then the forecasts are evaluated under the realized utility RU-framework (Bollerslev et al. (2018)) which mimics an investor who targets at constant Sharp ratio and rebalances the position according to the forecasts. The economic values evaluation confirms our findings. Such an investor would obtain up to 19 bps extra utility when changing from HAR to RSV in the long horizon case. While in the short horizon case, the utility of the investor increases up to 22 bps by using the simple HAR model. Lastly, the investor can employ BTC-D to diversify idiosyncratic jump risk and gain higher utility in the short horizon case.

# Appendix A.

## A.1. *RV Comparison*

**Table 7:** Summary Statistics of BTC Annualized Realized Variance Against Global Exchange Indices

|       | AEX <sup>†</sup> | DJI <sup>†</sup> | FTSE <sup>†</sup> | HSI <sup>†</sup> | SPX <sup>†</sup> | SSEC <sup>†</sup> | BTC-D | BTC-G |
|-------|------------------|------------------|-------------------|------------------|------------------|-------------------|-------|-------|
| count | 4 842            | 4 704            | 4 769             | 4 645            | 4 709            | 4 508             | 864   | 883   |
| mean  | 0.16             | 0.12             | 0.14              | 0.15             | 0.13             | 0.23              | 1.16  | 0.93  |
| std   | 0.38             | 0.30             | 0.32              | 0.41             | 0.32             | 0.46              | 2.05  | 1.76  |
| min   | 0.10%            | 0.08%            | 0.16%             | 0.35%            | 0.04%            | 0.23%             | 2.00% | 0.76% |
| 25%   | 0.02             | 0.02             | 0.02              | 0.03             | 0.02             | 0.03              | 0.08  | 0.04  |
| 50%   | 0.05             | 0.04             | 0.05              | 0.06             | 0.05             | 0.09              | 0.56  | 0.40  |
| 75%   | 0.14             | 0.11             | 0.13              | 0.14             | 0.12             | 0.23              | 3.70  | 3.17  |
| max   | 7.04             | 5.55             | 7.74              | 16.46            | 7.18             | 7.71              | 26.07 | 21.99 |

†: Selected global indices from developed markets and emerging markets. Trading hours in different global exchanges could be different which introduce bias of *RV*. We correct such bias by accounting the overnight price change (Bollerslev et al. (2018)) to allow those *RV* estimators to be comparable.

Datasource from Realized Library, Oxford-Man Institute of Quantitative Finance.



## A.2. Out-of-Sample Forecasts Evaluation and Economic Values from Squared Form Forecasting Models

**Table 8:** Adaptive HAR Model Out-of-Sample Forecasts Performance Evaluation

|                   | BTC-D |                    |                    |                    | BTC-G |                    |                    |                    |
|-------------------|-------|--------------------|--------------------|--------------------|-------|--------------------|--------------------|--------------------|
|                   | HAR   | RVJ                | RSV                | RSVSJ              | HAR   | RVJ                | RSV                | RSVSJ              |
| <b>h=1</b>        |       |                    |                    |                    |       |                    |                    |                    |
| MZ-R <sup>2</sup> | 0.267 | 0.248              | 0.285              | 0.165              | 0.213 | 0.182              | 0.226              | 0.151              |
| MSE               | 3.636 | 3.850              | 3.676              | 4.812 <sup>†</sup> | 2.437 | 2.508              | 2.411              | 2.872              |
| HRMSE             | 1.569 | 1.576              | 1.767 <sup>†</sup> | 1.756 <sup>†</sup> | 1.976 | 2.080              | 2.022              | 2.583 <sup>†</sup> |
| QLIKE             | 0.846 | 1.100 <sup>†</sup> | 0.988 <sup>†</sup> | 1.545 <sup>†</sup> | 0.749 | 1.636 <sup>†</sup> | 1.139 <sup>†</sup> | 4.706 <sup>†</sup> |
| <b>h=7</b>        |       |                    |                    |                    |       |                    |                    |                    |
| MZ-R <sup>2</sup> | 0.365 | 0.416              | 0.431              | 0.458              | 0.355 | 0.360              | 0.424              | 0.435              |
| MSE               | 1.643 | 1.437              | 1.573              | 1.272 <sup>*</sup> | 0.990 | 0.888              | 0.875 <sup>*</sup> | 0.818 <sup>*</sup> |
| HRMSE             | 1.359 | 1.278              | 1.455              | 1.279              | 1.278 | 1.366 <sup>†</sup> | 1.050 <sup>*</sup> | 1.624              |
| QLIKE             | 0.984 | 0.997              | 1.037              | 1.043              | 0.797 | 1.341 <sup>†</sup> | 0.878              | 1.738 <sup>†</sup> |
| <b>h=30</b>       |       |                    |                    |                    |       |                    |                    |                    |
| MZ-R <sup>2</sup> | 0.543 | 0.682              | 0.628              | 0.677              | 0.635 | 0.682              | 0.707              | 0.813              |
| MSE               | 0.673 | 0.462 <sup>*</sup> | 0.514 <sup>*</sup> | 0.440 <sup>*</sup> | 0.314 | 0.256 <sup>*</sup> | 0.235 <sup>*</sup> | 0.147 <sup>*</sup> |
| HRMSE             | 0.779 | 0.614 <sup>*</sup> | 0.698 <sup>*</sup> | 0.444 <sup>*</sup> | 0.696 | 0.554 <sup>*</sup> | 0.529 <sup>*</sup> | 0.404 <sup>*</sup> |
| QLIKE             | 0.937 | 0.898 <sup>*</sup> | 0.877 <sup>*</sup> | 0.874 <sup>*</sup> | 0.770 | 0.743 <sup>*</sup> | 0.722 <sup>*</sup> | 0.741              |

The table reports the out-of-sample forecasting performance of BTC-D (left part) and BTC-D (right part) in different forecasting horizons  $h = 1, 7, 30$  separated into three panels. The columns of each panel from left to right are HAR, RVJ, RSV, and RSVSJ models detailed in section 4.1. The rows of each panel from top to down are R<sup>2</sup> of Mincer-Zarnowitz forecasting regression, mean squared error, heteroscedasticity adjusted root mean squared error, and mean of gaussian quasi-likelihood error. The † marks when the HAR model outperforms significantly other models, while the \* denotes that the HAR model underperforms other models significantly, and the significance is confirmed by D-M test at 5% significant level. The forecasts are conducted in the squared forms and then used for the performance evaluation.

## A.3. Realized Utility Evaluation of Squared Form Forecasting Models

Note that the  $RU_{t+h}$  metric could be negative as shown in Table 9 where RSVSJ model produces negative utility of -1.843 in the case of  $h = 1$ . Reason for that is severe under-forecasting on  $RV_{t+1}$ , i.e  $RV_{t+1}/\widehat{RV}_{t+1}^{(m)} > 4$ .

**Table 9:** Economic Values Evaluation of Out-of-Sample Forecasts (%)

|             | BTC-D        |       |              |       | BTC-G        |       |              |        |
|-------------|--------------|-------|--------------|-------|--------------|-------|--------------|--------|
|             | HAR          | RVJ   | RSV          | RSVSJ | HAR          | RVJ   | RSV          | RSVSJ  |
| <b>h=1</b>  | <b>2.938</b> | 2.496 | 2.626        | 1.421 | <b>2.650</b> | 1.330 | 2.041        | -1.843 |
| <b>h=7</b>  | <b>3.071</b> | 3.048 | 2.916        | 2.874 | <b>3.164</b> | 1.862 | 2.906        | 1.100  |
| <b>h=30</b> | 3.569        | 3.642 | <b>3.708</b> | 3.678 | 3.585        | 3.637 | <b>3.689</b> | 3.621  |

The table reports the economic value gained in terms of realized utility of BTC-D (left part) and BTC-G (right part). The columns of each part from left to right are realized utility from four different models including HAR, RVJ, RSV, and RSVSJ model detailed in section 4.1. Each of the forecasting models is in squared form, and then the forecast is used to calculate the realized utility. The rows are realized utility in three different forecasting horizons,  $h = 1, 7, 30$ . The highest utility of each forecasting horizon is bolded for both BTC-D and BTC-G. All the realized utility are reported in percentage.

## Appendix B.

### B.1. Local Variance Estimation

We employ the nonparametric local variance estimate Fan and Yao (2008)

$$\widehat{V}_t^{[n]} = \frac{\sum_{i=-l, i \neq -1, 0, 1}^l K\left(\frac{i}{l}\right) \cdot r_{t+i}^2 \cdot \mathbf{I}\{r_{t+i}^2 \leq c_\theta^2 \cdot \widehat{V}_{t+i}^{[n-1]}\}}{\sum_{i=-l, i \neq -1, 0, 1}^l K\left(\frac{i}{l}\right) \cdot \mathbf{I}\{r_{t+i}^2 \leq c_\theta^2 \cdot \widehat{V}_{t+i}^{[n-1]}\}}, n = 1, 2, 3 \dots \quad (28)$$

Where  $K$  is a Gaussian kernel with bandwidth value  $l = 25$ . To avoid using future information and for computational simplicity,  $\widehat{V}_t$  is estimated within each day. Thus, the first and last  $l$ -points of  $\widehat{V}_t$  each day are smoothed by only partial Gaussian kernel. This recursive computation stops when the change from last step is smaller than a given criterion.

### B.2. Conditional Expected Return

The expected value of  $\eta$ -power returns conditioning on the square returns larger than threshold

$$\begin{aligned} r^e(\theta, \eta) &= \mathbb{E} \left\{ |r|^\eta \mid r^2 > \theta \right\} \\ &= \frac{(2\sigma^2)^{\frac{\eta}{2}}}{2\sqrt{\pi}\Phi\left(-\frac{\sqrt{\theta}}{\sigma}\right)} \cdot \Gamma\left(\frac{\eta+1}{2}, \frac{\theta}{2\sigma^2}\right) \end{aligned} \quad (29)$$

Given that the  $\sigma^2$  is approximated by  $\widehat{V}_t$ , we have:

$$r^e(\theta_t, \eta) = \frac{1}{2\sqrt{\pi}\Phi(-c_\theta)} \cdot \left(\frac{2\theta_t}{c_\theta^2}\right)^{\frac{\eta}{2}} \cdot \Gamma\left(\frac{\eta+1}{2}, \frac{c_\theta^2}{2}\right) \quad (30)$$

Where  $\Phi(x)$  is cdf of  $N(0,1)$  and  $\Gamma(\alpha, x) = \int_x^{+\infty} s^{\alpha-1} e^{-s} ds$  is the upper incomplete gamma function.

### B.3. Realized Utility

A first order expansion on expected utility yields (for  $h = 1$ )

$$\mathbb{E}[u(W_{t+1})] = \mathbb{E}(W_{t+1}) - \frac{1}{2}\gamma^A \mathbb{V}(W_{t+1}), \quad (31)$$

where  $\gamma^A$  is the absolute Pratt-Arrow risk aversion. The wealth function  $W$  is explicitly given by (32) for allocating  $\omega_t$  proportion of whole wealth on the risky asset, and  $r_{t+1} - r_f$  is the unknown excess return.

$$\begin{aligned} W_{t+1} &= W_t \{1 + (1 - \omega_t)r_f + \omega_t r_{t+1}\} \\ &= W_t \{1 + r_f + \omega_t(r_{t+1} - r_f)\} \end{aligned} \quad (32)$$

Assuming that the risk-free interest rate  $r_f$  is constant,  $W_t$  and  $\omega_t$  are known, the expected value and variance of  $W_{t+1}$  is:

$$\begin{aligned} \mathbb{E}(W_{t+1}) &= W_t(1 + r_f) + W_t\omega_t(r_{t+1} - r_f) \\ \mathbb{V}(W_{t+1}) &= W_t^2\omega_t^2 \cdot \mathbb{V}(r_{t+1} - r_f) \end{aligned} \quad (33)$$

Given a target Sharp ratio  $SR = \frac{\mathbb{E}(r_{t+1})}{\sqrt{\mathbb{V}(r_{t+1})}}$ , (33) and (31) give the following expression of expected utility  $EU(\omega_t)$  with replacing  $\mathbb{V}(r_{t+1})$  by  $RV_{t+1}$

$$\begin{aligned} EU(\omega_t) &= W_t \left[ \omega_t \mathbb{E}(r_{t+1}) - \frac{\gamma}{2}\omega_t^2 \mathbb{V}(r_{t+1}) \right] \\ &= W_t \left[ \omega_t \mathbb{E}(r_{t+1}) - \frac{\gamma}{2}\omega_t^2 RV_{t+1} \right] \\ &= W_t \left[ \omega_t \cdot SR \cdot \sqrt{RV_{t+1}} - \frac{\gamma}{2}\omega_t^2 RV_{t+1} \right] \end{aligned} \quad (34)$$

Here the  $\gamma = \gamma^A W_t$  represents the relative risk aversion. Based on the out-of-sample forecasts  $\widehat{RV}_{t+1}^{(m)}$  from model  $m$ , one can derive the optimal weight  $\omega_t^{(m)}$  targeting  $SR/\gamma$ .

$$\omega_t^{(m)} = \frac{SR/\gamma}{\sqrt{\widehat{RV}_{t+1}^{(m)}}} \quad (35)$$

The Realized Utility  $RU_{t+1}^{(m)}$  at time  $t + 1$  by model  $m$  defined as utility per wealth with optimal weights  $RU_{t+1}^{(m)} = EU(\omega_t^{(m)})/W_t$  can be obtained by (35) and (34).

$$RU_{t+1}^{(m)} = \frac{SR^2}{\gamma} \left( \sqrt{\frac{RV_{t+1}}{\widehat{RV}_{t+1}^{(m)}}} - \frac{1}{2} \frac{RV_{t+1}}{\widehat{RV}_{t+1}^{(m)}} \right) \quad (36)$$

## References

- Ait-Sahalia, Y., Mykland, P. A., Zhang, L., 2005. How often to sample a continuous-time process in the presence of market microstructure noise. *The Review of Financial Studies* 18, 351–416.
- Andersen, T. G., Bollerslev, T., Diebold, F. X., 2007. Roughing it up: Including jump components in the measurement, modeling, and forecasting of return volatility. *The Review of Economics and Statistics* 89, 701–720.
- Andersen, T. G., Bollerslev, T., Diebold, F. X., Ebens, H., 2001a. The distribution of realized stock return volatility. *Journal of Financial Economics* 61, 43–76.
- Andersen, T. G., Bollerslev, T., Diebold, F. X., Labys, P., 2001b. The distribution of realized exchange rate volatility. *Journal of the American Statistical Association* 96, 42–55.
- Balcilar, M., Bouri, E., Gupta, R., Roubaud, D., 2017. Can volume predict bitcoin returns and volatility? a quantiles-based approach. *Economic Modelling* 64, 74–81.
- Bandi, F. M., Russell, J. R., 2008. Microstructure noise, realized variance, and optimal sampling. *Review of Economic Studies* 75, 339–369.
- Barndorff-Nielsen, O. E., Hansen, P. R., Lunde, A., Shephard, N., 2008a. Designing realized kernels to measure the ex post variation of equity prices in the presence of noise. *Econometrica* 76, 1481–1536.
- Barndorff-Nielsen, O. E., Kinnebrock, S., Shephard, N., 2008b. Measuring downside risk-realised semivariance. CREATES Research Paper .
- Barndorff-Nielsen, O. E., Shephard, N., 2002a. Econometric analysis of realized volatility and its use in estimating stochastic volatility models. *Journal of the Royal Statistical Society: Series B (Statistical Methodology)* 64, 253–280.
- Barndorff-Nielsen, O. E., Shephard, N., 2002b. Estimating quadratic variation using realized variance. *Journal of Applied Econometrics* 17, 457–477.
- Barndorff-Nielsen, O. E., Shephard, N., 2004. Power and bipower variation with stochastic volatility and jumps. *Journal of Financial Econometrics* 2, 1–37.
- Barndorff-Nielsen, O. E., Shephard, N., 2006. Econometrics of testing for jumps in financial economics using bipower variation. *Journal of Financial Econometrics* 4, 1–30.

- Bollerslev, T., Ghysels, E., 1996. Periodic autoregressive conditional heteroscedasticity. *Journal of Business & Economic Statistics* 14, 139–151.
- Bollerslev, T., Hood, B., Huss, J., Pedersen, L. H., 2018. Risk everywhere: Modeling and managing volatility. *The Review of Financial Studies* 31, 2729–2773.
- Bouri, E., Molnár, P., Azzi, G., Roubaud, D., Hagfors, L. I., 2017. On the hedge and safe haven properties of bitcoin: Is it really more than a diversifier? *Finance Research Letters* 20, 192–198.
- Bukovina, J., Martiček, M., et al., 2016. Sentiment and bitcoin volatility. Tech. rep., Mendel University in Brno, Faculty of Business and Economics.
- Conrad, C., Custovic, A., Ghysels, E., 2018. Long-and short-term cryptocurrency volatility components: A garch-midas analysis. *Journal of Risk and Financial Management* 11, 23.
- Corsi, F., 2009. A simple approximate long-memory model of realized volatility. *Journal of Financial Econometrics* 7, 174–196.
- Corsi, F., Pirino, D., Reno, R., 2010. Threshold bipower variation and the impact of jumps on volatility forecasting. *Journal of Econometrics* 159, 276–288.
- Diebold, F. X., Mariano, R. S., 2002. Comparing predictive accuracy. *Journal of Business & Economic Statistics* 20, 134–144.
- Dyhrberg, A. H., 2016. Bitcoin, gold and the dollar – a GARCH volatility analysis. *Finance Research Letters* 16, 85–92.
- Fan, J., Yao, Q., 2008. *Nonlinear Time Series: Nonparametric and Parametric Methods*. Springer Science & Business Media.
- Fleming, J., Kirby, C., Ostdiek, B., 2001. The economic value of volatility timing. *The Journal of Finance* 56, 329–352.
- Garcia, D., Schweitzer, F., 2015. Social signals and algorithmic trading of bitcoin. *Royal Society open science* 2, 150288.
- Gerlach, J.-C., Demos, G., Sornette, D., 2019. Dissection of bitcoin’s multiscale bubble history from january 2012 to february 2018. *Royal Society Open Science* 6, 180643.
- Glaser, F., Zimmermann, K., Haferkorn, M., Weber, M. C., Siering, M., 2014. Bitcoin-asset or currency? revealing users’ hidden intentions. *Revealing Users’ Hidden Intentions* (April 15, 2014). ECIS .

- Griffin, J. M., Shams, A., 2018. Is bitcoin really un-tethered? Available at SSRN: <https://ssrn.com/abstract=3195066> .
- Gronwald, M., 2014. The economics of bitcoins—market characteristics and price jumps. Available at SSRN: <https://ssrn.com/abstract=2548999> .
- Hafner, C. M., 2018. Testing for bubbles in cryptocurrencies with time-varying volatility. *Journal of Financial Econometrics* .
- Hansen, P. R., Lunde, A., 2006. Realized variance and market microstructure noise. *Journal of Business & Economic Statistics* 24, 127–161.
- Hou, A. J., Wang, W., Chen, C. Y., Härdle, W. K., 2018. Pricing cryptocurrency options: The case of bitcoin and crix. Available at SSRN: <https://ssrn.com/abstract=3159130> .
- Huang, X., Tauchen, G., 2005. The Relative Contribution of Jumps to Total Price Variance. *Journal of Financial Econometrics* 3, 456–499.
- Liu, L. Y., Patton, A. J., Sheppard, K., 2015. Does anything beat 5-minute rv? a comparison of realized measures across multiple asset classes. *Journal of Econometrics* 187, 293–311.
- Mancini, C., 2009. Non-parametric threshold estimation for models with stochastic diffusion coefficient and jumps. *Scandinavian Journal of Statistics* 36, 270–296.
- Nakamoto, S., 2008. Bitcoin: A peer-to-peer electronic cash system .
- Nolte, I., Xu, Q., 2015. The economic value of volatility timing with realized jumps. *Journal of Empirical Finance* 34, 45–59.
- Patton, A. J., 2011. Volatility forecast comparison using imperfect volatility proxies. *Journal of Econometrics* 160, 246–256.
- Patton, A. J., Sheppard, K., 2015. Good volatility, bad volatility: Signed jumps and the persistence of volatility. *Review of Economics and Statistics* 97, 683–697.
- Pichl, L., Kaizoji, T., 2017. Volatility analysis of bitcoin price time series. *Quantitative Finance and Economics* 1, 474–485.
- Scaillet, O., Treccani, A., Trevisan, C., 2018. High-Frequency Jump Analysis of the Bitcoin Market\*. *Journal of Financial Econometrics* .

- Swanson, N. R., White, H., 1997. Forecasting economic time series using flexible versus fixed specification and linear versus nonlinear econometric models. *International Journal of Forecasting* 13, 439–461.
- Traian Pele, D., Niels, W., Härdle, W. K., Kolossiatis, M., Yatracos, Y., 2019. Phenotypic convergence of cryptocurrencies. IRTG 1792 Discussion Paper .
- Trimborn, S., Härdle, W. K., 2018. Crix an index for cryptocurrencies. *Journal of Empirical Finance* 49, 107–122.
- Urquhart, A., Zhang, H., 2019. Is bitcoin a hedge or safe haven for currencies? an intraday analysis. *International Review of Financial Analysis* 63, 49–57.
- Yermack, D., 2015. Is bitcoin a real currency? an economic appraisal. In: *Handbook of digital currency*, Elsevier, pp. 31–43.
- Zhang, L., 2006. Efficient estimation of stochastic volatility using noisy observations: A multi-scale approach. *Bernoulli* 12, 1019–1043.
- Zhang, L., Mykland, P. A., AÃt-Sahalia, Y., 2005. A tale of two time scales. *Journal of the American Statistical Association* 100, 1394–1411.